Molecular Structure and Pseudorotation of 1,1-Dichlorocyclopentane As Determined by Gas-Phase Electron Diffraction and ab Initio Calculations: A Large Amplitude Treatment

Marwan Dakkouri,*,† Volker Typke,*,‡ and Tilman Schauwecker†

Department of Electrochemistry and Communication and Information Center, University of Ulm, D-89069 Ulm, Germany

Received: October 16, 2003; In Final Form: March 17, 2004

The molecular structure of 1,1-dichlorocyclopentane (DClCP) has been investigated by means of gas-phase electron diffraction and ab initio calculations. Although the electron diffraction data could be fairly well reproduced by a C_s (envelope) model we found it more pertinent to apply a pseudorotation model to account for the dynamic and large amplitude motion in DClCP. On the basis of this model we analyzed the dependency of the ring geometric parameters and vibrational mean amplitudes on the phase angle ϕ. For a better elucidation of this distinct dependency we developed particular equations which describe the dependency of the distribution of the delocalized net charges throughout the ring on the phase angle ϕ. The joint electron diffraction and ab initio study has led to the following r_a structural parameters of DClCP (C_s conformer): $r(C-Cl)_{ax} = 1.787(3)$ Å, $r(C-Cl)_{eq} = 1.769(3)$ Å, average $r(C-C)_{ring} = 1.535(1)$ Å, $r(C-H)_{av} = 1.114(5)$ Å, $\angle(C5-C1-C2) = 103.0(9)°$, $\angle(Cl-C-Cl) = 108.6(3)°$, and $\angle(H-C-H) = 104.6(26)°$. The puckering amplitude for the five-membered ring was determined to be $q = 0.400(11)$ Å. The quantum mechanical calculations were carried out by utilizing the Hartree−Fock, density functional B3PW91, and perturbation MP2 methods and applying the following basis sets: cc-pVDZ, 6-31G(d,p), 6-311G(df,pd), 6-311+G(d,p), 6-311++G(d,p), 6-311+G(2df,2pd), and 6-311++G(2df,2pd). For the purpose of comparison and systematic study, we optimized the geometries and calculated the charge distributions using the natural population analysis (NPA) and Mulliken population analysis (MPA) of 1,1-difluorocyclopentane, 1,1-dibromocyclopentane, and their corresponding monohalogenated derivatives.

Introduction

In a very recent study[1] we analyzed the structure of 1,1-dicyanoycyclopentane and investigated the hindered pseudorotational motion in this five-membered-ring molecule. Various intriguing features emerged from this study and among them was the noticeable dependency of the geometry parameters, vibrational amplitudes, and charge distribution on the phase angle ϕ.

These interesting results have prompted us to study one further geminally substituted cyclopentane with substituents possessing different electronic properties than the cyano groups. Accordingly, we investigated the structure of 1,1-dichlorocyclopentane (DClCP) by means of electron diffraction and ab initio calculations. Static one-conformer (C_s and C_1 forms) and two-conformer (C_s plus C_2) models as well as a model considering the pseudorotational motion have been used to fit the experimental data.

The main perspectives for conducting the present work are as follows: (1) to obtain additional relevant results which may contribute to a more complete and perhaps detailed understanding of the hindered pseudorotational motion in five-membered rings; (2) to explore the influence of the geminal chlorine atoms on the pseudorotational parameters of the five-membered ring, the phase angle ϕ, and the puckering amplitude q; and (3) from the comparison of the structural and pseudorotational parameters in 1,1-dicyanocyclopentane and DClCP to deduce whether there is some certain correlation between the nature of the geminal substituents and these parameters.

Synthesis and Experimental Data

Synthesis. The sample of 1,1-dichlorocyclopentane was prepared by the reaction of phosphorus pentachloride with cyclopentanone following a modified route of Domnin et al.[2] We used benzene as a solvent instead of ligroin and performed the reaction at 10 °C instead of 0 °C. Furthermore, to prevent the formation of monochlorocyclopentene the cyclopentanon-benzene solution was added very slowly (one drop per 5 s) to the PCl_5/benzene slurry and the entire reaction was carried out under anhydrous conditions by applying a stream of dry nitrogen. The subsequent decomposition of $POCl_3$ was undertaken very carefully at about 5 °C and under vigerous stirring. The crude product was purified by using a 100 cm spinning band column. The main fraction was obtained at 51 °C/30 Torr ($n_D^{25} = 1.4685$). Further purification was carried out by using gas chromatography separation. To ascertain the purity of the sample, IR and mass spectra were taken.

The gas-phase electron diffraction intensities were recorded on Kodak Electron Image plates with a Balzers KD-G2 diffraction unit at the University of Tübingen. The accelerating voltage was 60 keV, and the recording temperature was about 30 °C. Data were collected at camera distances of 50 and 25 cm (nominal) yielding molecular intensity values at intervals (Δs) of 0.2 Å^{-1} ranging from $s = 1.6$ to 17.6 Å^{-1} and from 9.0 to 33.8 Å^{-1}. The electron wavelength was calibrated with ZnO diffraction patterns giving $\lambda_{500} = 0.049243 \pm 0.000058$ Å and

† Department of Electrochemistry.
‡ Communication and Information Center.

10.1021/jp031172w CCC: $27.50
Published on Web 05/04/2004

TABLE 1: Optimized Geometrical Parameters of 1,1-Dichlorocyclopentane (DClCP) and 1,1-Difluorocyclopentane (DFCP) As Predicted by Different Levels of Theory

	DClCP				DFCP			
	C_s symmetry		C_2 symmetry		C_s symmetry		C_2 symmetry	
parameter	B3PW91 /6-311 +G(df,pd)	MP2 /6-311 +G(2df,2pd)	B3PW91 /6-311 +G(df,pd)	MP2 /6-311 +G(2df,2pd)	B3PW91 /6-311 +G(df,pd)	MP2 /6-311 +G(2df,2pd)	B3PW91 /6-311 +G(df,pd)	MP2 /6-311 +G(2df,2pd)
bond distances (Å)								
C_1-C_2	1.522	1.519	1.542	1.541	1.516	1.509	1.530	1.525
C_2-C_3	1.536	1.535	1.529	1.527	1.536	1.534	1.530	1.528
C_3-C_4	1.553	1.554	1.529	1.528	1.556	1.557	1.532	1.531
q[a]	0.395	0.419	0.421	0.450	0.370	0.400	0.403	0.432
$C_1-Cl(F)_6$	1.811	1.794	1.806	1.790	1.375	1.373	1.370	1.368
$C_1-Cl(F)_7$	1.792	1.776	1.806	1.790	1.363	1.360	1.370	1.368
$\langle C-H\rangle$[b]	1.091	1.088	1.092	1.089	1.091	1.087	1.092	1.089
bond angles (deg)								
$C_1-C_2-C_3$	103.8	103.2	104.7	104.1	103.7	102.8	104.7	104.2
$C_2-C_3-C_4$	105.9	105.7	102.8	102.0	106.2	105.9	103.1	102.4
$C_5-C_1-C_2$	103.9	103.5	106.4	106.3	105.6	105.4	107.4	107.5
Cl(F)−C−Cl(F)	108.4	109.0	107.6	108.1	105.8	106.4	105.2	105.7
$H-C_2-H$	108.0	108.5	107.8	108.3	108.2	108.8	108.1	108.6
$H-C_3-H$	107.1	107.4	107.6	108.1	106.8	107.2	107.4	107.9
β_6[c]	122.7	122.1	126.2	126.0	123.8	122.8	127.4	127.2
β_7[d]	128.8	129.0	126.2	126.0	130.4	130.9	127.4	127.2
α[e]	39.8	42.3			37.7	40.1		
dihedral angles (deg)								
$C_1-C_2-C_3-C_4$	23.9	25.3	−35.1	−37.3	22.4	24.1	−33.5	−35.7
$C_4-C_5-C_1-C_2$	39.3	41.7	13.4	14.3	37.2	40.4	12.8	13.7
$C_2-C_3-C_4-C_5$	0.0	0.0	43.6	46.5	0.0	0.0	41.6	44.4
μ[f]	2.73	2.76	2.84	2.88	2.68	2.83	2.75	2.92

[a] Puckering amplitude for the ring, calculated with the program RING.[12,13] [b] Average value. [c] Angle between the bond $Cl(F)_6-C_1$ and the plane $C_5C_1C_2$. [d] Angle between the bond $Cl(F)_7-C_1$ and the plane $C_5C_1C_2$. [e] Angle between the $C_5C_1C_2$ plane and $C_2C_3C_4C_5$ plane (flap angle). [f] Dipole moment.

$\lambda_{250} = 0.049376 \pm 0.000046$ Å. Optical densities from three photographic plates for both distances were recorded on our computer-controlled and -modified microdensitometer ELSCAN E-2500 (Optronics International, Chelmsford, MA). Our usual data reduction and refinement procedures were used,[3,4] and the atomic scattering amplitudes and phases of Haase[5] were applied. The intensity data used for the determination of the molecular structure are provided in the Supporting Information.

Ab initio Calculations

The quantum mechanical computations were carried out on various levels of theory, using the programs Gaussian98,[6] Spartan,[7] and MOLPRO.[8] The following computational procedures were applied: HF/cc-pVDZ, HF/6-31G(d,p), HF/6-311+G(d,p), density functional (DFT) hybrid B3PW91/6-311+G(df,pd), and Møller−Plesset perturbation method MP2 in combination with the basis sets 6-311G(d,p), 6-311+G(d,p), 6-311++G(d,p), 6-311+G(2df,2pd), and 6-311++G(2df,2pd). It should be pointed out, however, that the augmentation of these basis sets by adding diffuse functions and higher polarization functions on both heavy atoms and hydrogen does not significantly affect the structural results. It remains to note that all these methods, particularly the perturbation methods, provided results, which are in good agreement with the experiment.

In the course of our systematic study of the effect of substituents and to examine whether certain correlations exist between the kind of substituent and structural and/or conformational changes we also performed ab initio calculations on the following related molecules: monofluorocyclopentane (MFCP), monochlorocyclopentane (MClCP), monobromocyclopentane (MBrCP), 1,1-difluorocyclopentane (DFCP), and 1,1-dibromocyclopentane (DBrCP). For more proper comparison of the results, all calculations were conducted with the same theoretical methods and basis sets that have been applied in the case of DClCP. For brevity reasons the results obtained for DBrCP and MBrCP have not been listed in the tables incorporated in this paper.

Tables 1 and S1 (S indicates Supporting Information) display the most prominent structural parameters for DClCP as predicted by the quantum mechanical methods which have been applied. For atomic numbering see Figure 1.

Pseudorotation

Saturated five-membered rings are known to undergo a special form of vibrational motion, the pseudorotation.[9−11] A close examination of the variation of nonbonded distances during one cycle of pseudorotation shows that in DClCP the intramolecular distances for several pairs of atoms change by up to 2 Å. This indicates that the analysis of electron diffraction patterns with a large amplitude treatment of the pseudorotation should be more appropriate than a static model allowing only for C_s symmetry. To apply this concept various problems have to be solved. Most importantly the dependency of the geometry on the phase angle ϕ must be analyzed because it is required to establish the ring geometry for any phase angle ϕ. Inspection of Tables 1 and S1 shows that the ring C−C bond distances as obtained from all ab initio methods for the C_s and C_2 conformers depend strongly on the phase angle ϕ: the C1−C2 distance increases by about 0.021 Å in going from $\phi = 0$ to $\pi/2$ and thereby the C3−C4 distance decreases by 0.024 Å. These changes in atomic distances are easily observable in the analysis of electron diffraction patterns.

In 1,1-disubstituted five-membered rings the pseudorotational motion is not a virtually free motion, but is characterized by a

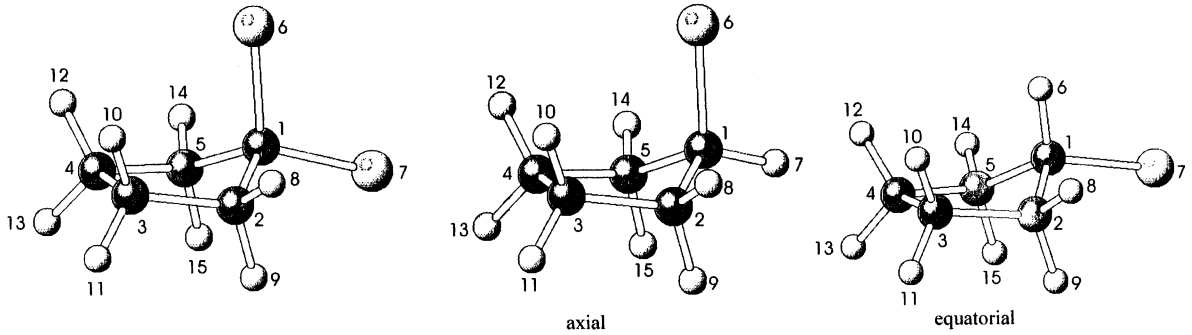

Figure 1. Atomic numbering of 1,1-dichlorocyclopentane (DClCP) and monochlorocyclopentane (MClCP).

hindering potential function of the form (neglecting higher terms)

$$V(\phi) = {}^1/_2V_2(1 - \cos2\phi) + {}^1/_2V_4(1 - \cos4\phi) + {}^1/_2V_6(1 - \cos6\phi) \quad (1)$$

where ϕ is the phase of the pseudorotation. This gives stable configurations of C_s symmetry at $\phi = 0, \pm\pi, \pm2\pi, ...$, and configurations of C_2 symmetry at $\phi = \pm\pi/2, \pm3\pi/2, ...$ It depends on the actual values of the coefficients whether the configurations of C_2 symmetry are stable or not. The energy difference between configurations of C_s and C_2 symmetry is given by $V_2 + V_6$.

To get reasonable estimates for the potential parameters V_2, V_4, and V_6, additional calculations with the program MOLPRO and the HF/cc-pVDZ method have been performed. Basically, the potential function $V(\phi)$ can be calculated by optimizing $3N - 7 = 38$ geometrical parameters for a number of configurations with a fixed value of the phase angle ϕ. Unfortunately the geometrical parameters used in the available ab initio programs for setting up the **Z** matrix do not allow for an immediate description of the pseudorotation. Therefore we tried to fix one of the dihedral angles which were used to locate the ring C atoms at values in a suitable range while the remaining parameters were optimized. Subsequently, we applied the program RING[12,13] to evaluate the corresponding puckering amplitude q and phase angle ϕ. It turns out that no such dihedral angle can be used to cover the full range in going from C_s symmetry to C_2 symmetry. Also, the resulting structures do not necessarily represent the configuration of lowest energy at given values of ϕ and q. Therefore we calculated the energy hypersurface in the following way: the program MOLPRO provides a mode to optimize the geometry on the basis of Cartesian coordinates and thereby fixing selected coordinates to some deliberately chosen value. We decided to fix the x-coordinate of atom C_1 to zero, and to fix the z-coordinates of all ring C atoms to a value calculated from the formula given by Kilpatrick et al.[14]

$$z_i = \sqrt{2/5}\, q \cos(\phi + 4\pi(i - 1)/5) \qquad (i = 1, ..., 5) \quad (2)$$

This leaves $3N - 6$ Cartesians to be adjusted in the geometry optimization. We varied the puckering amplitude q in a reasonable range with a step width of 0.01 Å, and ϕ with a step width of 10° in the range 90° to 270°. The results of these calculations are shown in Figure 3. The line indicating the bottom of the energy valley corresponds to the minimum energy at a given value of the phase angle ϕ, and it also gives the optimal puckering amplitude q at this ϕ. It turns out that q is not constant during one cycle of pseudorotation. Subsequently the calculated values for the energy were analyzed to derive the coefficients of the potential function $V(\phi)$. We found that the coefficient V_6 is required to adequately describe the calculated energy values. The same analysis was also performed for the puckering amplitude with a formula similar to eq 1:

$$q(\phi) = q_0 + q_2 \cos2\phi + q_4 \cos4\phi + q_6 \cos6\phi \qquad (3)$$

In Table 2 are collected the minimum values of the puckering amplitude $q_{min}(\phi)$ and the relative energy $E_{min}(\phi) = E(\phi \neq 180°) - E(\phi = 180°)$ at distinct values of ϕ as well as the derived coefficients of eqs 1 and 3. Figure 2 shows the potential function for 1,1-dichlorocyclopentane as obtained with the HF/cc-pVDZ method and the calculated energy values. The points marked "×" are obtained assuming a constant puckering amplitude q for all phase angles ϕ.

From the calculations described above it is obvious that the molecular structure is available for the complete cycle of pseudorotation. This offers the possibility to analyze the deformation of the ring due to the pseudorotation. Following the approach we presented in a previous paper[1] we applied a model which assumes that the density distribution of the delocalized net charges, which represents the overall distribution of charges throughout the ring, depends markedly on the phase angle ϕ. Assuming that this dependency can be described by a function, d, of the form shown in Figure 4 we write for the density distribution

$$d(\alpha, \phi) = d_1 \cos\alpha + d_2 \cos2\alpha + d_{c2c} \cos\alpha \cos2\phi + d_{s2s} \sin\alpha \sin2\phi + d_{c4c} \cos\alpha \cos4\phi + d_{s4s} \sin\alpha \sin4\phi + d_{2c2c} \cos2\alpha \cos2\phi + d_{2s2s} \sin2\alpha \sin2\phi + d_{2c4c} \cos2\alpha \cos4\phi + d_{2s4s} \sin2\alpha \sin4\phi \quad (4)$$

where α designates the angle between the axis from the center of the ring to atom C_1 and every position along the ring, both projected to the mean plane as defined by Cremer and Pople.[13] The coefficients d_1, d_2, etc. are adjustable parameters. Compared to the relatively simple formula given previously,[1] eq 4 includes more terms to cover the values of all ring C−C bond distances during one cycle of pseudorotation. With this density function we now write for the contribution of the delocalized net charges to the bond distance C_i−C_j

$$r_{ij} = r_{CC} + \int_{\alpha_i}^{\alpha_j} d(\alpha,\phi)\, d\alpha \qquad (5)$$

Assuming a regular pentagon in the mean plane of the five-membered ring the integral can be easily evaluated. If we adjust the parameters r_{CC}, d_1, d_2, etc. to the ab initio distances by

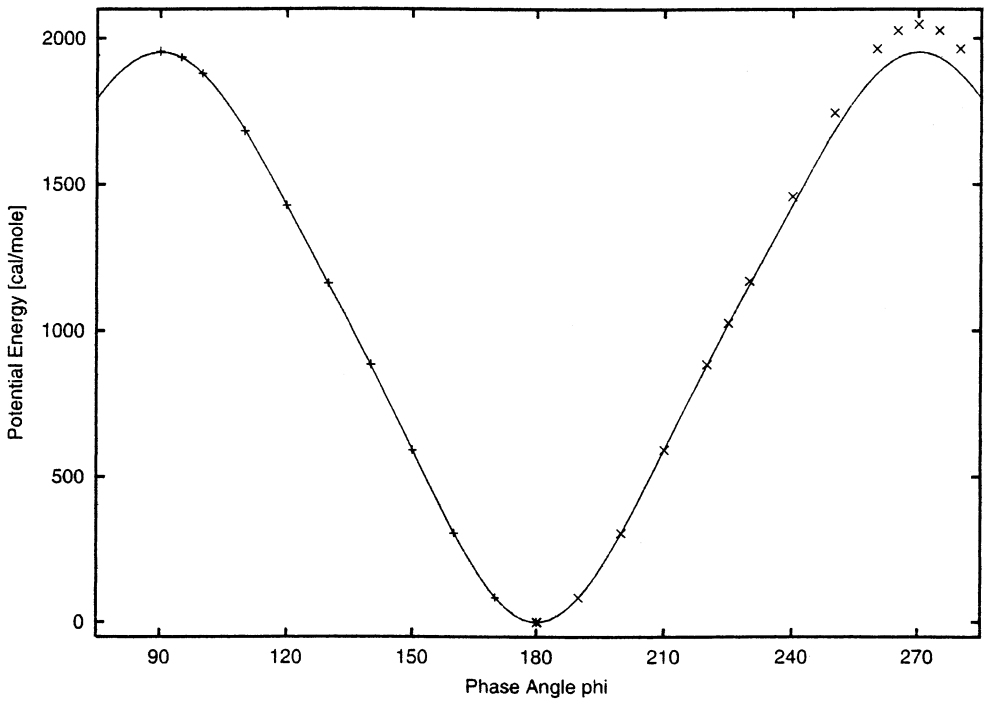

Figure 2. Potential function of pseudorotation for 1,1-dichlorocyclopentane as obtained from calculations with the method HF/cc-pVDZ. Points "+" are obtained as the minimum of the calculated energies at constant ϕ, points "×" are obtained with the assumption of constant q in the theoretical calculations.

TABLE 2: Minimum Value of the Relative Energy (cal/mol) and Puckering Amplitude q (Å) at Various Values of Phase Angle ϕ

phase	q_{min}	E_{min}
90	0.423	1955.6
95	0.422	1935.9
100	0.421	1879.1
110	0.417	1681.3
120	0.410	1428.1
130	0.402	1161.5
140	0.396	883.5
150	0.393	590.1
160	0.393	304.6
170	0.394	84.5
180	0.395	0.0

V	q
$V_2 = 1860.6$	$q_0 = 0.4038$
$V_4 = 44.7$	$q_2 = -0.0151$
$V_6 = 93.3$	$q_4 = 0.0051$
	$q_6 = 0.0012$

TABLE 3: Fitted Constants from Eq 4 for 1,1-Dichlorocyclopentane

parameter	value	parameter	value
r_{CC}	1.5369		
d_1	0.0027	d_2	0.0008
d_{c2c}	0.0107	d_{c2c}	−0.0002
d_{s2s}	0.0097	d_{2s2s}	−0.0009
d_{c4c}	−0.0004	d_{2c4c}	0.0020
d_{s4s}	−0.0009	d_{2s4s}	0.0026

applying a least-squares procedure we obtain the results shown in Table 3. It can be easily verified from eq 5 that r_{CC} is the mean value of the ring C−C bond distances. Combining the values of the integrals and the constants from Table 3 we find that the ring C−C bond distances vary as

$$r_{ij} = r_{CC} + \delta r_{ij} + c_{2,ij}\cos(2\phi) + c_{4,ij}\cos(4\phi) \pm s_{2,ij}\sin(2\phi) \pm s_{4,ij}\sin(4\phi) \quad (6)$$

TABLE 4: Fourier Coefficients for the Ring C−C Bond Distances (Eq 6) and the C−C−C Bond Angles (Eq 7)

parameter	r_{12},r_{15}	r_{23},r_{45}	r_{34}
δr_{ij}	−0.0024	0.0004	0.0040
$c_{2,ij}$	−0.0102	0.0041	0.0123
$c_{4,ij}$	0.0010	−0.0017	0.0014
$s_{2,ij}$	−0.0075	−0.0104	0.0
$s_{4,ij}$	0.0030	−0.0004	0.0
parameter	α_{123},α_{451}	α_{234},α_{345}	α_{512}
$\alpha_{0,ijk}$	104.24	104.57	105.29
$c_{2,ijk}$	−0.29	1.54	−1.27
$c_{4,ijk}$	0.03	−0.18	−0.18
$c_{6,ijk}$	−0.06	0.01	0.00
$s_{2,ijk}$	−1.27	−1.26	0.0
$s_{4,ijk}$	−0.06	0.18	0.0
$s_{6,ijk}$	−0.02	−0.01	0.0

The coefficients of this equation have been included in Table 4, and Figure 5 shows the variation of the ring C−C bond distances with the phase angle ϕ and the correlation with the density of the delocalized net charge within these bonds.

The deformation of the ring is further characterized by the changes in the C−C−C bond angles. It is interesting to note that the changes of these angles reflect the variation in the density of the net charge at the apex atom as calculated from eq 4 in the same way as the C−C bond distances do. In Figure 6 we show the correlation between the variation of the bond angles C−C−C and of the fluctuation of the delocalized charge density at the apex atom as a function of the phase angle ϕ. A Fourier analysis of the calculated C−C−C bond angles according to the equation

$$\alpha_{ijk} = \alpha_{0,ijk} + c_{2,ijk}\cos2\phi + c_{4,ijk}\cos4\phi + c_{6,ijk}\cos6\phi \pm s_{2,ijk}\sin2\phi \pm s_{4,ijk}\sin4\phi \pm s_{6,ijk}\sin6\phi \quad (7)$$

yields the coefficients collected in Table 4.

It is also interesting to analyze the variation of geometrical parameters with the phase angle ϕ involving ligands attached

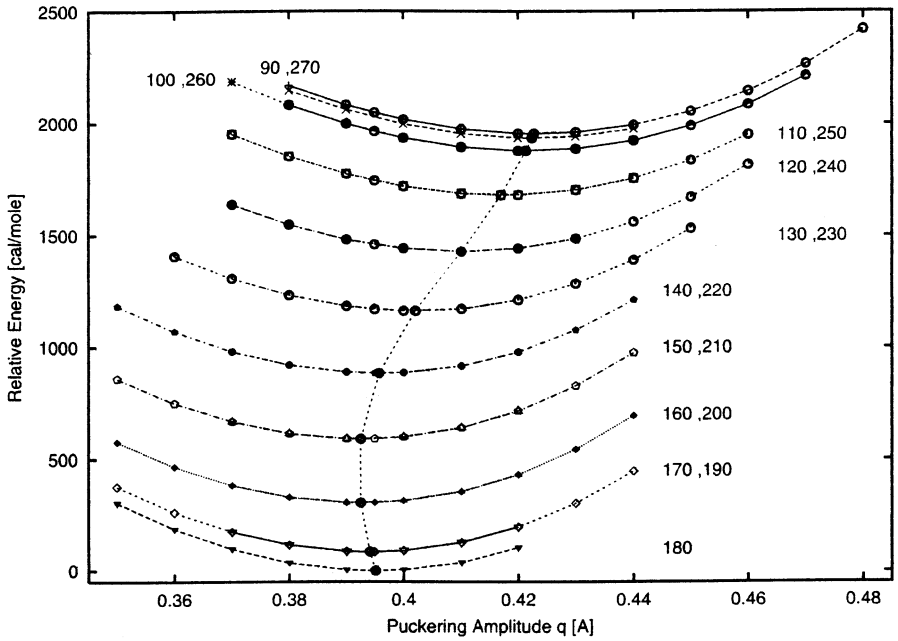

Figure 3. Calculated relative energies (cal/mol) of 1,1-dichlorocyclopentane at different values of puckering amplitude q and phase angle ϕ (angles in deg). Parameters at the curves are the corresponding values of the phase angle ϕ.

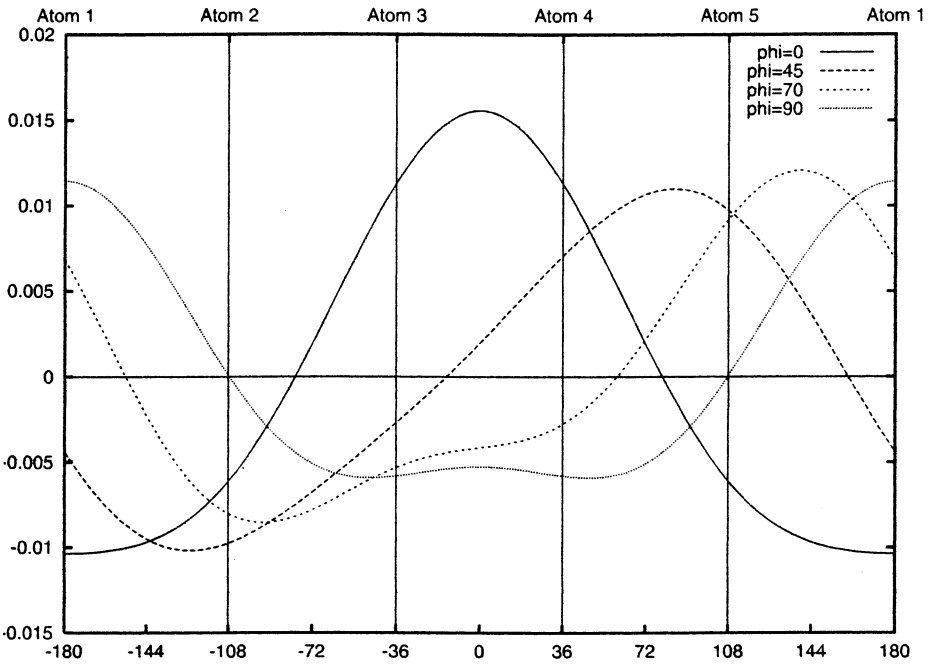

Figure 4. Density of delocalized net charge distribution eq 4 for $\phi = 0°$, 45°, 70°, and 90°.

to the ring C atoms. There are two types of parameters to be studied: alterations of the bond distances and bond angles. With regard to the angle deformations one has to keep in mind that there are redundancies relating the angles at atoms with four bonds, and also the ring C−C−C angles are not all independent. We choose to analyze the rocking (ρ), wagging (ω), and twisting (τ) angles as defined by Skancke et al.[15] in addition to the ring C−C−C angles and the Cl−C−Cl and H−C−H angles.

We start by analyzing the variation of the parameters involving the Cl atoms. We found that the C−Cl bond lengths are well reproduced by the equation

$$r_{CCl} = R_0 \pm R_1 \cos\phi + R_2 \cos 2\phi \pm R_3 \cos 3\phi + R_4 \cos 4\phi \tag{8}$$

This formula is valid for both the axial and the equatorial positions of the C−Cl bond: the upper sign corresponds to the C−Cl_6 bond, the lower sign to the C−Cl_7 bond (cf. Figure 1). In Table 5 the coefficients R_0 through R_4 are listed, and in Figure 7 we show the correlation between the C−Cl bond distances and the charge density at atom C_1.

Next we investigate the dependency of the angle β = Cl−C−Cl on the phase angle ϕ. It turns out that this angle varies by only 0.7°. However, it is more interesting to note that the rocking, wagging, and twisting angles change more drastically. The Fourier analysis of the calculated values of all these geometrical parameters results in the following functions:

$$\beta(\phi) = \beta_0 + \beta_2 \cos 2\phi + \beta_4 \cos 4\phi + \beta_6 \cos 6\phi$$

$$\rho(\phi) = \rho_1 \cos\phi + \rho_3 \cos 3\phi + \rho_5 \cos 5\phi$$

$$\omega(\phi) = \omega_2 \sin2\phi + \omega_4 \sin4\phi + \omega_6 \sin6\phi$$

$$\tau(\phi) = \tau_1 \sin\phi + \tau_3 \sin3\phi + \tau_5 \sin5\phi \quad (9)$$

Table 5 also includes the resulting coefficients β_0 through τ_5 and the corresponding functions are shown in Figure 7.

Finally we examined the deformations of the CH_2 groups during half a cycle of the pseudorotation. It is interesting to note that all C−H distances can be represented by two formulas: one for the distances at the C_2 and C_5 atoms and the other for the distances at the C_3 and C_4 atoms. Only the signs of the coefficients are different for each C−H bond. Similarly the H−C−H bond angles and the rocking, wagging, and twisting angles are represented by the following formulas

$$r_{C_{2,5}H} = r_{2,0} \pm r_{2,c1}\cos\phi \pm r_{2,c2}\cos2\phi \pm r_{2,c3}\cos3\phi \pm r_{2,c4}\cos4\phi \pm r_{2,s1}\sin\phi \pm r_{2,s2}\sin2\phi \pm r_{2,s3}\sin3\phi \pm r_{2,s4}\sin4\phi$$

$$r_{C_{3,4}H} = r_{3,0} \pm r_{3,c1}\cos\phi \pm r_{3,c2}\cos2\phi \pm r_{3,c3}\cos3\phi \pm r_{3,c4}\cos4\phi \pm r_{3,s1}\sin\phi \pm r_{3,s2}\sin2\phi \pm r_{3,s3}\sin3\phi \pm r_{3,s4}\sin4\phi$$

$$\beta_{HC_{2,5}H} = \beta_{2,0} + \beta_{2,c2}\cos2\phi + \beta_{2,c4}\cos4\phi \pm \beta_{2,s2}\sin2\phi \pm \beta_{2,s4}\sin4\phi$$

$$\beta_{HC_{3,4}H} = \beta_{3,0} + \beta_{3,c2}\cos2\phi + \beta_{3,c4}\cos4\phi + \beta_{3,c6}\cos6\phi \pm \beta_{3,s2}\sin2\phi \pm \beta_{3,s4}\sin4\phi \pm \beta_{3,s6}\sin6\phi$$

$$\rho_{C_{2,5}H} = \rho_{2,c1}\cos\phi + \rho_{2,c3}\cos3\phi + \rho_{2,c5}\cos5\phi \pm \rho_{2,s1}\sin\phi \pm \rho_{2,s3}\sin3\phi \pm \rho_{2,s5}\sin5\phi$$

$$\rho_{C_{3,4}H} = \rho_{3,c1}\cos\phi + \rho_{3,c3}\cos3\phi + \rho_{3,c5}\cos5\phi \pm \rho_{3,s1}\sin\phi \pm \rho_{3,s3}\sin3\phi \pm \rho_{3,s5}\sin5\phi$$

$$\omega_{C_{2,5}H} = \pm\omega_{2,0} \pm \omega_{2,c2}\cos2\phi \pm \omega_{2,c4}\cos4\phi \pm \omega_{2,c6}\cos6\phi + \omega_{2,s2}\sin2\phi + \omega_{2,s4}\sin4\phi + \omega_{2,s6}\sin6\phi$$

$$\omega_{C3,4H} = \pm\omega_{3,0} \pm \omega_{3,c2}\cos2\phi \pm \omega_{3,c4}\cos4\phi \pm \omega_{3,c6}\cos6\phi + \omega_{3,s2}\sin2\phi + \omega_{3,s4}\sin4\phi + \omega_{3,s6}\sin6\phi$$

$$\tau_{C_{2,5}H} = \pm\tau_{2,c1}\cos\phi \pm \tau_{2,c3}\cos3\phi \pm \tau_{2,c5}\cos5\phi + \tau_{2,s1}\sin\phi + \tau_{2,s3}\sin3\phi + \tau_{2,s5}\sin5\phi$$

$$\tau_{C_{3,4}H} = \pm\tau_{3,c1}\cos\phi \pm \tau_{3,c3}\cos3\phi \pm \tau_{3,c5}\cos5\phi + \tau_{3,s1}\sin\phi + \tau_{3,s3}\sin3\phi + \tau_{3,s5}\sin5\phi \quad (10)$$

The coefficients in these formulas are displayed in Table 6 and the changes in the geometry are shown in Figure 8 for the groups $H_8-C_2-H_9$ and $H_{10}-C_3-H_{11}$; the corresponding representations for the remaining CH_2 groups are obtained simply by rotating the figures by 180°.

Static Models

We started the analysis of the electron diffraction data by applying static models of C_s symmetry and C_2 symmetry. Since not all independent structural parameters of DClCP can be determined from the electron diffraction intensities, initially a number of simplifying assumptions had to be introduced for the data refinement. However, with the availability of the ab initio results it became evident that most of these assumptions were quite poor. In particular it turned out to be important to take into account the differences of the ring C−C bond distances, the rocking of the CH_2 groups, and the difference of the C−Cl bond distances in the case of the C_s symmetry. Improving the structural models in this way it soon became apparent that in analogy to 1,1-dicyanocyclopentane[1] the experimental intensities for DClCP are best reproduced by using the envelope form (C_s symmetry), but not the C_2 conformation, when the static model was employed. The predominance of the C_s form is consistent with the results predicted by all ab initio methods that have been applied for this study (Tables 1 and S1).

TABLE 5: Deformation of the CCl_2 Group with Phase Angle ϕ: The Fourier Coefficients of the Geometrical Parameters (Eq and 9)

order	R	β	ρ	ω	t
0	1.8030	107.66	0.0	0.0	0.0
1	−0.0111	0.0	7.23	0.0	0.10
2	−0.0020	0.34	0.0	1.26	0.0
3	0.0022	0.0	−1.59	0.0	−0.47
4	−0.0004	0.10	0.0	−0.71	0.0
5	0.0	0.0	0.40	0.0	0.18
6	0.0	0.02	0.0	0.08	0.0

Since the energy values which were obtained from the ab initio calculations at various levels of theory have shown (Table 7) that some contribution of the C_2 conformer to the diffraction intensities cannot be excluded, we also applied a two-conformer model and fitted the ratio of the two conformers. In the latter calculations it proved to be important to additionally take into account the changes of the geometrical parameters and vibrational amplitudes in going from the C_s to the C_2 symmetry. To limit the number of geometrical parameters the calculations were finally performed by using the dependency of the geometrical parameters on ϕ, as described in the previous chapter, with ϕ restricted to 180° (C_s) and 90° (C_2).

To obtain reliable starting values for the vibrational amplitudes l_{ij} we carried out a normal coordinate analysis. All calculations were based on the results of the ab initio calculations, using the HF/6-31G** method for the C_s and C_2 conformers. The procedure we applied for the determination of these amplitudes has been described previously.[16] It is worthwhile to note that initially the values for several calculated vibrational amplitudes of nonbonded distances were unreasonably large. The subsequent elimination of the contributions originating from the lowest vibrational frequency, however, has led to generally plausible values.

The final results of the structural analysis gained from the refinement of the one or two conformer static models are shown in Table 8.

However, all calculations described above gave results which were not fully satisfying, particularly in the region between 3 and 5 Å of the radial distribution function (cf. Figures10 and 11). As can be seen from Figure 11 this is the region with the strongest dependency of the radial distribution function on the phase angle ϕ. This prompted us to start a large-amplitude treatment of the geometry of DClCP. Such a treatment can be done by fitting a dynamic model similar to what we described previously[1] for 1,1-dicyanocyclopentane. A detailed description of an extended treatment is reported in the next section. Another method of treatment is to fit an "effective" structure by using a static model of C_1 symmetry. Fitting such a model can be achieved by adding the phase angle ϕ as a free parameter. This model improves the agreement between the experimental and theoretical radial distribution function within the range between

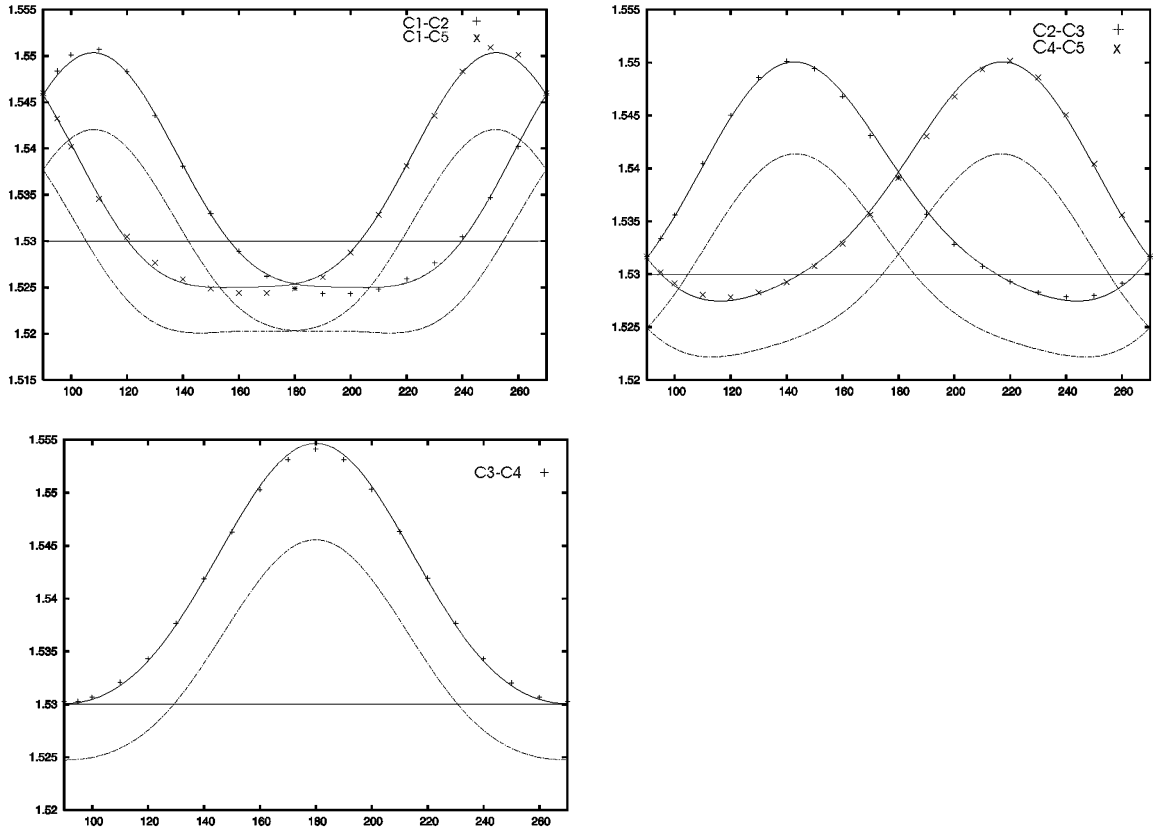

Figure 5. Variation of the ring C−C bond distances and density of delocalized net charge (-•-) with the phase angle ϕ. The density function was shifted upward by 1.53 to fit into the figure.

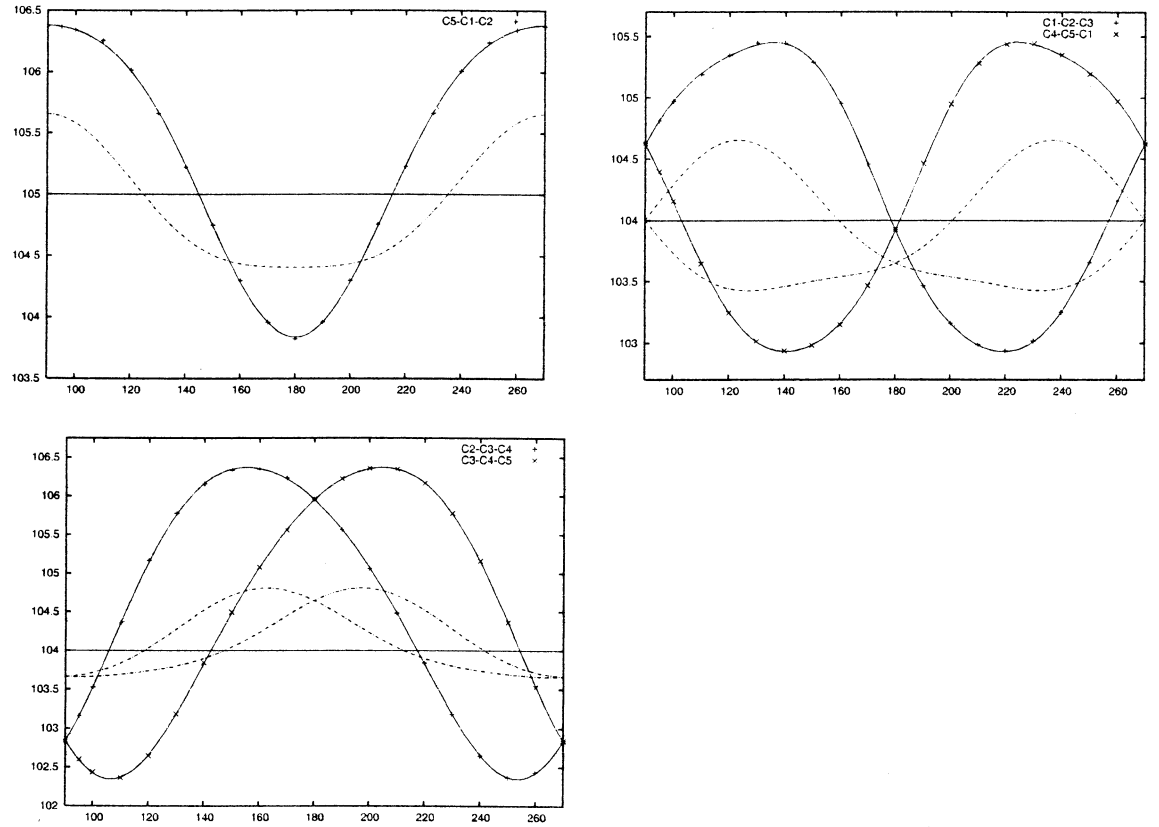

Figure 6. Variation of the ring C−C−C bond angles and density of delocalized net charge (-•-) at the apex atoms with the phase angle ϕ. The density function was scaled by 57.3 and shifted upward by 104° or 105° to fit into the figure.

TABLE 6: Deformation of the CH_2 Groups with Phase Angle ϕ: Fourier Coefficients of the Geometrical Parameters (Eq 10)

		sign of coefficient for the bond			
name	coefficient	C_2-H_8	C_2-H_9	C_5-H_{14}	C_5-H_{15}
$r_{2,0}$	1.0887	+	+	+	+
$r_{2,c1}$	0.0021	+	-	+	-
$r_{2,c2}$	0.0009	+	+	+	+
$r_{2,c3}$	0.0003	-	+	-	+
$r_{2,c4}$	0.0000	-	-	-	-
$r_{2,s1}$	0.0010	+	-	-	+
$r_{2,s2}$	0.0014	+	+	-	-
$r_{2,s3}$	0.0000	+	-	-	+
$r_{2,s4}$	0.0002	-	-	+	+

		sign of coefficient for the bond			
name	coefficient	C_3-H_{10}	C_3-H_{11}	C_4-H_{12}	C_4-H_{13}
$r_{3,0}$	1.0908	+	+	+	+
$r_{3,c1}$	0.0004	+	-	-	+
$r_{3,c2}$	0.0011	-	-	-	-
$r_{3,c3}$	0.0000	-	+	+	-
$r_{3,c4}$	0.0002	+	+	+	+
$r_{3,s1}$	0.0011	-	+	-	+
$r_{3,s2}$	0.0001	-	-	+	+
$r_{3,s3}$	0.0004	+	-	+	-
$r_{3,s4}$	0.0001	-	-	+	+

order	$\beta_{HC_{2,5}H}$	$\rho_{HC_{2,5}H}$	$\omega_{C_{2,5}H}$	$\tau_{C_{2,5}H}$	$\beta_{HC_{3,4}H}$	$\rho_{HC_{3,4}H}$	$\omega_{C_{3,4}H}$	$\tau_{C_{3,4}H}$
0	107.95	0.0	−4.99	0.0	107.32	0.0	−1.00	0.0
C1	0.0	−9.58	0.0	−0.49	0.0	0.77	0.0	−0.83
C2	0.06	0.0	−0.78	0.0	−0.29	0.0	−0.18	0.0
C3	0.0	0.44	0.0	−1.18	0.0	1.19	0.0	−0.89
C4	0.03	0.0	0.19	0.0	0.02	0.0	−0.18	0.0
C5	0.0	0.05	0.0	0.03	0.0	0.14	0.0	0.10
C6	0.0	0.0	0.0	0.0	0.01	0.0	−0.03	0.0
S1	0.0	−6.03	0.0	0.68	0.0	5.69	0.0	−0.88
S2	0.44	0.0	−0.18	0.0	0.27	0.0	−0.34	0.0
S3	0.0	1.90	0.0	−0.74	0.0	0.40	0.0	1.19
S4	0.01	0.0	0.21	0.0	−0.01	0.0	−0.03	0.0
S5	0.0	−0.20	0.0	0.16	0.0	−0.10	0.0	−0.03
S6	0.0	0.0	−0.05	0.0	0.01	0.0	0.01	0.0

3 and 5 Å. The results of the calculations from applying a static model of C_1 symmetry have been included in Table 8.

Large-Amplitude Treatment

To account for large-amplitude motions in the analysis of gas-phase electron diffraction data the assumption is made that the large-amplitude motion is a slow motion, and the reduced total molecular intensity $s\cdot M(s)$ can be written as[17,18]

$$s\cdot M(s)_{\text{total}} = \int_0^{2\pi} w(\phi)\, s\cdot M(s,R(\phi))\, \mathrm{d}\phi / \int_0^{2\pi} w(\phi)\, \mathrm{d}\phi \qquad (11)$$

where $R(\phi)$ designates the geometry of the molecule at the phase angle ϕ. The weight function $w(\phi)$ at temperature T with normalizing factor N is given by

$$w(\phi) = N\mathrm{e}^{-V(\phi)/RT} \qquad (12)$$

In principle nine independent structural parameters are required to calculate the positions of the atoms in a five-membered ring with no symmetry. We chose the 5 C−C bond distances, the bond angles $C_5-C_1-C_2$ and $C_1-C_2-C_3$, the puckering amplitude q, and the phase angle ϕ from the pseudorotational model. Utilizing eq 2 and setting $x_1 = 0$, the Cartesian coordinates of all ring atoms can be calculated. Though this involves the solution of three quadratic equations there is normally no difficulty in selecting the solutions which suit the above parameters. To set up the molecular geometry at a selected value of the phase angle ϕ additional use was made of eqs 3, 6, and 7. However, not all coefficients in these equations can be refined to fit the electron diffraction patterns. We decided to fix the higher order Fourier coefficients at the values displayed in Tables 2 and 4. This leaves the parameters r_{CC}, q_0, $\alpha_{0,512}$, and $\alpha_{0,123}$ as adjustable parameters of the ring geometry. In the fitting process it turned out that the parameter $\alpha_{0,123}$ could not be adjusted reasonably. Therefore, this parameter was maintained at a value that enforced the C_s symmetry at $\phi = 180°$.

Similarly the dependency of the geometry of the CCl_2 and CH_2 groups on the phase angle ϕ was taken into account by applying eqs 8−10. Again the zeroth order parameters (R_0, β_0) and one first-order parameter (ρ_1) were taken as adjustable parameters for the CCl_2 group, and for the CH_2 groups the mean values $(r_{2,0} + r_{3,0})/2$ and $(\beta_{2,0} + \beta_{3,0})/2$ were used. The higher order coefficients were taken from Tables 5 and 6.

A second problem to be solved is the correlation between the root-mean-square amplitudes l_{ij} and the phase angle ϕ. Using the scaled quadratic ab initio force fields for both conformations C_s and C_2 we have calculated the vibrational amplitudes within the range $\pi/2 \le \phi \le 3\pi/2$ with a step width of $\delta\phi = 9°$. Hilderbrandt et al.[19,20] tried to establish a dependency of the vibrational amplitudes on ϕ of the form

$$l_{ij} = l_{ij}^{\,0} + a(1 - \cos\phi)$$

where a is a constant. However, a detailed analysis of some selected vibrational amplitudes shows that the dependency of,

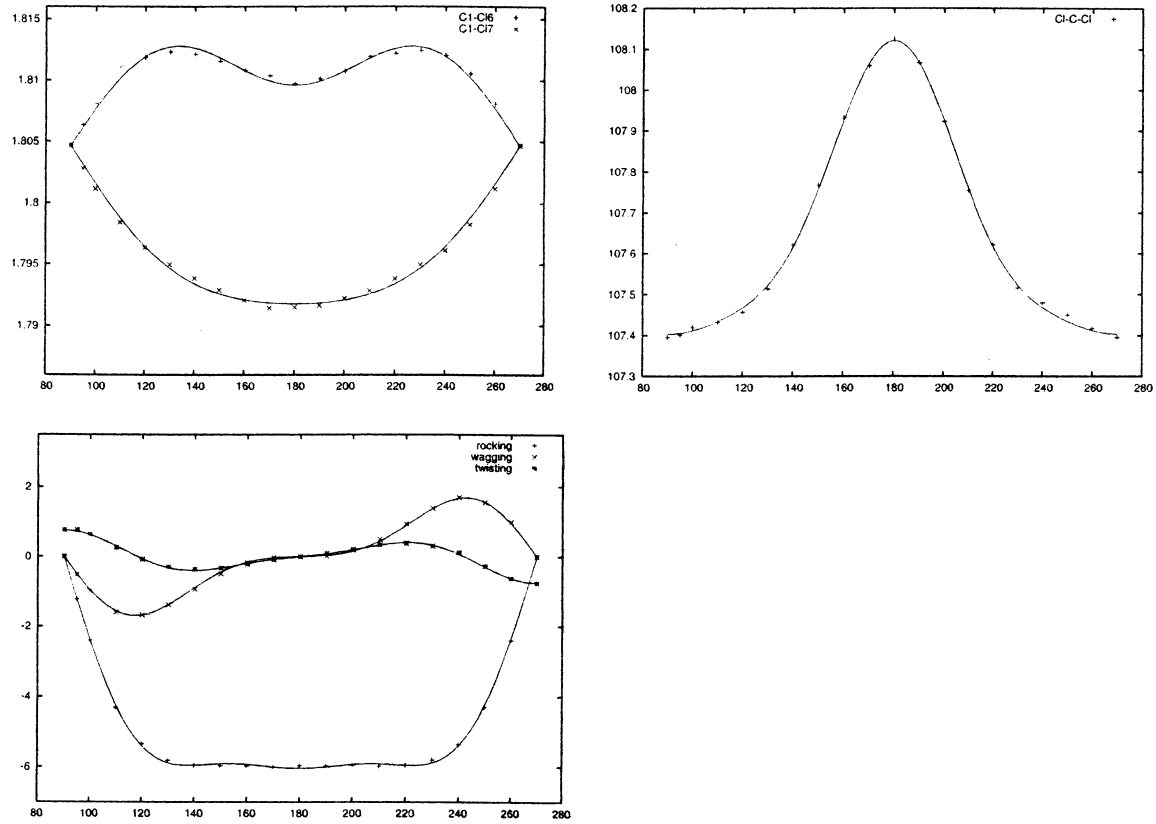

Figure 7. Deformation of the CCl_2 group dependent on the phase angle ϕ.

e.g., the vibrational amplitude $l(Cl_6...H_{10})$ on ϕ is of the form

$$l_{6,10} = l_0 + c_1(1 - \cos\phi) + c_2(1 - \cos 2\phi) + c_3(1 - \cos 3\phi) + c_4(1 - \cos 4\phi) + s_1(1 - \sin\phi) + s_2(1 - \sin 2\phi) + s_3(1 - \sin 3\phi) + s_4(1 - \sin 4\phi)$$

Therefore, as described in a previous paper,[1] we preferred to use the differences $l_{ij}(\phi \neq 180°) - l_{ij}(\phi = 180°)$ of the calculated vibrational amplitudes: these were introduced into the analyzing programs as constants to be added to the vibrational amplitudes of the most stable conformer (symmetry C_s at $\phi = 180°$). This limits the possibility of adjusting the vibrational amplitudes in the least-squares procedure to cases where the fluctuation of the calculated amplitudes is sufficiently small. Values at intermediate ϕ were obtained by interpolation.

To calculate $s \cdot M(s)_{total}$ from eq 11 we used the usual assumption that the integral can be appoximated sufficiently well by finite sums. Therefore, the geometry of the molecule was set up at various values of the phase angle ϕ, and the corresponding $M(s,R(\phi))$ was calculated. For symmetry reasons it is sufficient to use an interval width of π. Actually, we used a step width of $\delta\phi = 5°$ in the interval $90° \leq \phi \leq 270°$, giving a total of 37 intermediate conformers.

No attempts have been undertaken to extract the potential constants V_2, V_4, and V_6 from the experimental gas electron diffraction data. Instead these constants were fixed at the values given in Table 2.

The fitted structural parameters and most important vibrational amplitudes resulting from the large-amplitude treatment are included in Table 8. In this table the different σ values have the following meaning: σ_1 is the single standard error of the fitting procedure, σ_2 is the propagated error resulting from the estimated uncertainties of the fixed parameters, and σ_{tot} is the total error estimate. The method we used to calculate the propagated error σ_2 and the total error σ_{tot} has been described elsewhere.[16,21] Figure 9 shows the experimental and theoretical reduced molecular intensity $s \cdot M(s)$ and Figure 10 the experimental and theoretical radial distribution function from the pseudorotational model.

It should be noted that the values in Table 8 correspond to the r_a representation of the molecular structure. The data required to convert the r_a representation into the r_α representation are available as Supporting Information (Table S2). For details about r_a, r_α, and other representations see for instance Kuchitsu and Cyvin.[22]

Table 9 shows a comparison of the bond distances, bond angles, and dihedral angles which have been obtained from the electron diffraction study and by using eqs 3 and 6−10 with $\phi = 90°$ (C_2 symmetry) and $\phi = 180°$ (C_s symmetry) with those obtained from the ab initio calculations at the MP2/6-311+G-(2df,2pd) level.

Discussion

The most interesting result of the theoretical calculations for DClCP is the differences in the ring C−C bond distances and their dependency on the actual configuration. As can be seen in Tables 1 and S1 the C_1-C_2 bond distance increases and the C_3-C_4 bond distance decreases on the order of 0.02 Å in going from the C_s to the C_2 conformation. In contrast, the decrease of the C_2-C_3 bond length is only on the order of 0.008 Å. These variations of the ring C−C bond distances are consistent not only for all computational methods which have been applied in this work, but also for all other 1,1-disubstituted derivatives of cyclopentane investigated thus far (Tables 1 and 10, and ref 1). To rationalize this observation we assume that the variation of the geometry is due to the variation of the overall density distribution of charges throughout the ring with the phase angle ϕ of the pseudorotational motion. Therefore the constants of

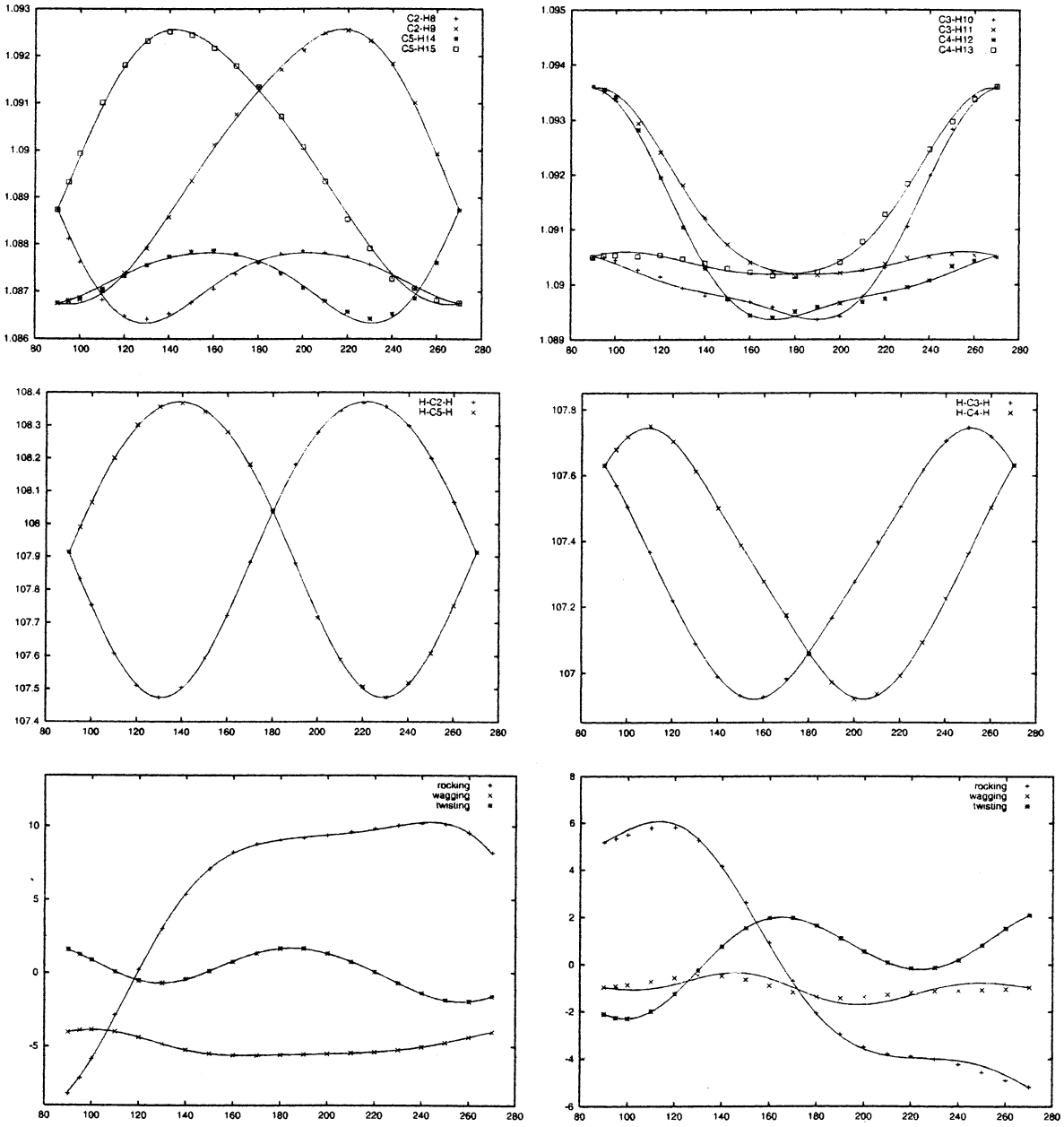

Figure 8. Dependency of geometrical parameters in the CH_2 groups on the phase angle ϕ: upper row, C_2-H and C_3-H distances; middle row, bond angles $H_8-C_2-H_9$ and $H_{10}-C_3-H_{11}$; lowest row, rocking, wagging, and twisting angles of the $H_8-C_2-H_9$ and $H_{10}-C_3-H_{11}$ groups.

TABLE 7: Energy Difference $\Delta E = E_{eq} - E_{ax}$ (kcal/mol) for MFCP, MClCP, MBrCP, Monocyanocyclopentane (MCCP), and Monoethynylcyclopentane (MECP) and $\Delta E = E_{C_2} - E_{C_s}$ for DFCP, DClCP, and DBrCP from ab Initio Calculations on Various Levels of Theory

method	MFCP	MClCP	MBrCP	MCCP	MECP	DFCP	DClCP	DBrCP
HF/cc-pVDZ							1.96	
HF/6-31G(d,p)							2.10	
B3LYP/6-311+G(df,pd)	1.17	0.48	0.28	−0.47	−0.73	−0.46	1.72	1.82
MP2/6-311G(d,p)	1.55	0.82	0.75	0.41	0.58	−0.19	2.75	3.14
MP2/6-311+G(d,p)					0.39	−0.15	2.77	
MP2/6-311++G(d,p)			0.85	0.53		−0.20	2.72	3.05
MP2/6-311+G(df,pd)	1.45	1.04	0.77			−0.08	2.88	3.13
MP2/6-311++G(df,pd)	1.44	1.20	0.84		0.51	−0.11	2.84	3.10
MP2/6-311+G(2df,2pd)	1.62	1.08	0.90	0.37	0.50	−0.30	2.38	
MP2/6-311++G(2df,2pd)	1.62	1.18				−0.32	2.35	

the function $d(\alpha,\phi)$ (eq 4) introduced in the section Pseudorotation were adjusted such that the ring C−C bond distances obtained at various values of ϕ and q_{min} are optimally reproduced. In Figure 4 the integral of the curve for $\phi = 0°$ (C_s symmetry, solid line) between atom 3 and atom 4 is clearly positive: this indicates a reduction in the density of the net charge between these atoms resulting in the long C_3-C_4 bond distance of 1.554 Å (Table S1, HF/cc-pVDZ method). On the other hand, the respective integral between atom 1 and atom 2 is negative resulting in the short C_1-C_2 bond distance of 1.525

TABLE 8: Final Model Parameters (r_a) and Errors for 1,1-Dichlorocyclopentane As Obtained from the Fit of Static Models and the Pseudorotation Model[a]

	static models			pseudorotation model			
	C_s	$C_s + C_2$	C_1	value	σ_1[m]	σ_2[n]	σ_{tot}[o]
	geometrical parameters (distances in Å, angles in deg)						
r_C[b]	1.534(2)	1.535(2)	1.535(2)	1.535	0.0005	0.0004	0.001
q_0[c]	0.397(12)	0.404(13)	0.405(14)	0.409	0.0042	0.0020	0.011
R_0[d]	1.781(2)	1.781(2)	1.781(2)	1.780	0.0007	0.0002	0.002
r_{CH}[e]	1.115(8)	1.114(6)	1.114(7)	1.114	0.0021	0.0001	0.005
$\alpha_{0,512}$[f]	105.7(11)	104.9(11)	105.4(9)	104.4	0.33	0.13	0.8
ϕ[g]	180.0(fix)	90.0/180.0 (fix)	161.3(11)				
β_0[h]	107.6(4)	107.9(4)	107.8(4)	108.1	0.12	0.04	0.3
β_{HCH}[i]	103.5(30)	104.1(31)	103.1(33)	104.6	1.03	2.22	2.6
ρ_1[j]	8.1(20)	8.1(19)	10.1(33)	10.0	0.67	0.31	1.7
	fitted vibrational amplitudes (Å)						
l(C−C)	0.053(2)	0.053(2)	0.052(2)	0.053	0.0006	0.0001	0.002
l(C−Cl)	0.056(3)	0.056(2)	0.056(2)	0.056	0.0008	0.0002	0.002
l(C−H)	0.090(7)	0.091(6)	0.089(6)	0.090	0.0020	0.0000	0.005
l(C···C)	0.059(5)	0.060(5)	0.058(5)	0.060	0.0015	0.0017	0.005
l(C···H_1)	0.101(10)	0.103(9)	0.102(9)	0.103	0.0030	0.0005	0.007
l(C···Cl_1)	0.078(19)	0.077(5)	0.074(24)	0.075	0.0021	0.0009	0.005
l(C···Cl_2)	0.173(16)	0.142(15)	0.130(54)	0.112	0.0046	0.0039	0.013
l(C···.Cl_3)	0.084(7)	0.079(8)	0.084(7)	0.078	0.0022	0.0006	0.006
l(Cl···Cl)	0.078(6)	0.077(6)	0.077(6)	0.076	0.0019	0.0008	0.005
% C_s		94.2(52)					
R_{long}[k]	5.01	4.55	4.61	4.44			
R_{short}[k]	7.78	7.22	7.55	7.15			
$\sum$[l]	0.0419	0.0352	0.0385	0.0345			

[a] Errors in parentheses (static models, in units of last digit) are three times the standard errors of the fit; for errors of the pseudorotational model see text. The fitted parameters are the zeroth and first-order coefficients defined in eqs 3 and 6−10. The higher order coefficients given in Tables 2−6 were used. [b] Constant term of the ring C−C bond distances (eq 6). [c] Constant term of the puckering amplitude (eq 3). [d] Constant term of the bond distances C−Cl (eq 8). [e] Constant term of the C−H bond distances (eq 10): $r_{CH} = (r_{2,0} + r_{3,0})/2$. [f] Constant term of the angle $C_5-C_1-C_2$ (eq 7). [g] Phase angle of pseudorotation. [h] Constant term of the angle Cl−C−Cl (eq 9). [i] Constant term of the H−C−H angles (eq 10): $\beta_{HCH} = (\beta_{2,0} + \beta_{3,0})/2$. [j] First Fourier coefficient of the rocking angle of the Cl−C−Cl group at C_s symmetry (eq 9). [k] $R = [\sum w_i\Delta_i^2/\sum(w_i s^2 M_i^2(\text{obs}))]^{1/2}$, where $\Delta_i = sM_i(\text{obs}) - sM_i(\text{calc})$. [l] $\sum$ is the weighted sum of squared residuals. [m] σ_1 is the single standard error of the fit. [n] σ_2 is the propagated error (see refs 16 and 21). [o] $\sigma_{tot} = [6\sigma_1^2 + 3\sigma_2^2]^{1/2}$

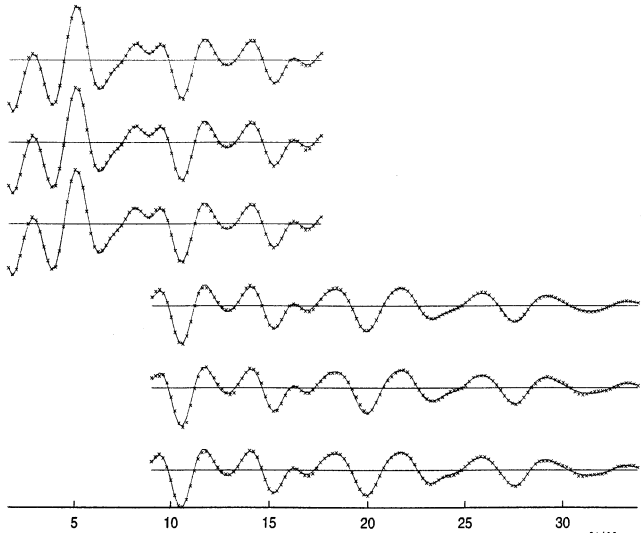

Figure 9. Experimental (×) and theoretical (−) reduced molecular intensity $s\cdot M(s)$ for DClCP.

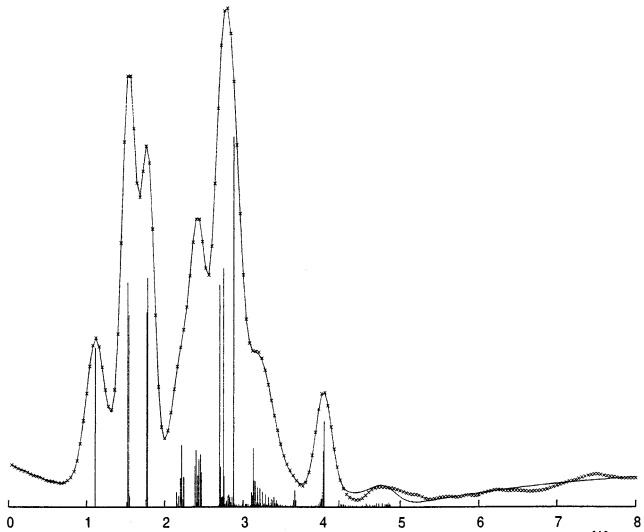

Figure 10. Experimental (×) and theoretical (−) radial distribution function from the pseudorotational model for DClCP.

Å. In the same way the curve for $\phi = 90°$ (C_2 symmetry, dotted line) shows that the distances C_2-C_3 and C_3-C_4 are very similar while the bond distance C_1-C_2 is long. Similar results were also obtained for DCCP.[1] We also note that the bond angles C−C−C are correlated with the variation of the charge density at the apex atom: this is demonstrated in Figure 6.

One further interesting result of the investigation of the pseudorotation is the curvature of the valley $E_{min}(\phi)$ and the corresponding puckering amplitude $q_{min}(\phi)$ as shown in Figure 3. A Fourier analysis shows that terms up to 6th order are required to satisfactorily reproduce the dependency on ϕ.

As can be seen from Figure 7, the deformation of the CCl2 group shows an unexpected form. Clearly the local minimum of the axial C−Cl bond distance at $\phi = 180°$, the opening of the Cl−C−Cl bond angle, and the almost constant value of the rocking angle over the range of about 100° are correlated with the variation of the charge density at atom 1.

The following remarks emerge from a closer inspection of

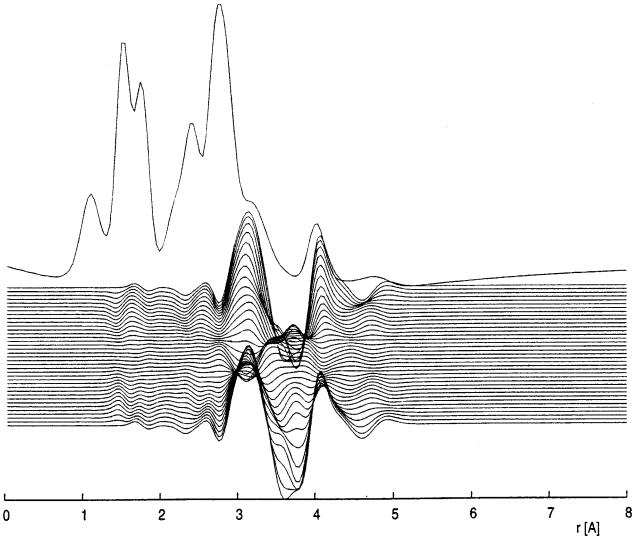

Figure 11. Theoretical total radial distribution function and differences between the contributions from the distinct conformations ($\phi = 90°$ through 270°) and the total radial distribution function for DClCP.

the results which were obtained from the electron diffraction analysis and are shown in Table 8:

First, we note that a one- or two-conformer statical model describes the experimental data surprisingly well. This obseravtion is clearly indicated by the value of $\sum$, the sum of weighted squared residuals of the fit. Obviously the quality of the fit can be slightly improved by releasing the restrictions imposed by enforcing C_s symmetry in favor of C_1 symmetry. A rather better description is achieved by allowing for a two-conformer model with C_s and C_2 symmetry. Therefore it is reasonable that the pseudorotational model, which in our case allows for 37 conformers, leads to a further improvement of the fit.

Second, the results for the one-conformer model of C_1 symmetry can well be taken as an "effective" structure. The intramolecular distances obtained for this model compare very well with the average of the distances obtained from all configurations with the phase angle ϕ taken from the interval $\pi/2 \leq \phi \leq \pi$, and using the weight function eq 12. A similar "effective" structure has been defined in the treatment of the internal rotation of methyl groups.[23]

Third, consideration of the results in Table 9 reveals that there is good agreement between the values of the parameters obtained from the various types of experimental analysis. Equally good is the consistency between the theoretically predicted values and those which have been determined from the experiment. Perhaps the C−Cl and C−H bond distances and the angles Cl−C−Cl and H−C−H represent some exceptions.

Some years ago Loyd, Mathur, and Harmony (LMH)[24] and Groner, Lee, and Durig (GLD)[25] investigated the microwave spectrum of monochlorocyclopentane (MClCP). In 1982 Hilderbrandt and Shen (HS)[19] also studied the conformation and structure of MClCP by applying the electron diffraction technique. All these investigations revealed that MClCP exists in the envelope C_s form with the chlorine atom either in the axial or in the equatorial position. Consistently, it also has been found that the axial conformer is slightly more stable than the equatorial form. As can be seen from Table 7, this finding is clearly supported by all ab initio procedures we employed in this work. While both the microwave[24] and the electron diffraction[19] studies provided only an average C−C bond length of 1.553(5) and 1.542(1) Å, respectively, the microwave investigation[25] presented three different bond distances for the ring C−C bonds in the axial conformer of C1−C2 = 1.544(8) Å, C2−C3 = 1.551(13) Å, and C3−C4 = 1.525(22) Å. From Table 10 it is apparent that the average of the predicted values by the MP2/6-311+G(df,pd) method for the C−C bond lengths is by 0.017 and 0.006 Å smaller than was obtained by LMH[24] and HS,[19] respectively. Moreover, the disagreement between the different C−C bond distances which have been presented by GLD[25] and those shown in Table 10 is significantly large. It is perhaps worth noting that the experimentally observed average C−C bond length is 0.018 Å shorter in DClCP (Table 8) than in MClCP.[24] This difference is most likely due to the overestimation of the ring C−C bond distances in MClCP and not the result of the disubstitution in DClCP. Furthermore, the observed C−Cl bond length in MClCP of 1.810 Å[19] agrees quite well with the predicted value of 1.800 Å (Table 10).

There is a notably good agreement between the theoretically predicted and experimentally determined values for the bond angles in MClCP. In the MW studies[24,25] it was found that the angles between the C−Cl bond and the C2−C1−C5 plane, the C2−C3−C4 angle, and the puckering angle are 123.5°, 105.8°, and 40.6°, and 124.8°, 106.7°, and 41.6°, respectively. From Table 10 it is apparent that the predicted values for these angles are 122.8°, 105.6°, and 41.0°.

It is perhaps of interest that we observe a direct relationship between the puckering amplitude q and the flap angle α for the envelope C_s conformation of the form:

$$\alpha/q = \sigma_s$$

where σ_s is a constant. We checked the validity of this simple formula for a series of geminally and monosubstituted (axial and equatorial) cyclopentanes and found that $\sigma_s \approx 100$ Å^{-1} for all those cyclopentanes which we studied in this work by means of quantum mechanical methods of the type cp-X (where X = HF, HCl, HBr, F_2, Cl_2, and Br_2). Only the σ_s value of 102 Å^{-1} for DFCP deviates slightly from this magnitude. Another exception is provided by 1,1-dicyanocyclopentane (DCCP) and monocyanocyclopentane (MCCP) which we studied previously.[1] Both compounds possess a σ_s value of 98 Å^{-1}. On the basis of these results it is conceivable that a certain series of compounds possesses its own specific value of σ_s. It remains to note that the σ_s value resulting from the experimental data for DClCP (Table 9) is also 100(4) Å^{-1}. Assuming a general validity of this relationship it can be postulated with some reservation that applying this equation would allow for the prediction of either the puckering amplitude or the flap angle for a wide range of substituted cyclopentanes.

It also should be added that a similar relationship has been observed for the C_2 (half-chair) conformer:

$$\tau/q = \sigma_2$$

where τ is the twist angle $C_2-C_3-C_4-C_5$ and σ_2 is a constant. For those compounds we investigated so far by means of computational methods, it turned out that $\sigma_2 = 103$ Å^{-1}. Should such a relationship prove to be applicable to many other substituted cyclopentanes this would permit the prediction of either q or τ.

In all mono- and disubstituted cyclopentane molecules we studied in the present work it has been observed that the axial carbon−halogen bond is always longer than the equatorial one. The MP2/6-311+G(2df,2pd) calculations for instance suggest for DClCP and MClCP (axial and equatorial) a bond length difference of 0.017 Å, and for DFCP and MFCP 0.012 and 0.013 Å (Tables 1 and 10), respectively. Loyd et al.[24] tried more or

TABLE 9: Comparison of r_a Distances, Bond Angles, and Dihedral Angles of 1,1-Dichlorocyclopentane (DClCP) at $\phi = 90°$ and 180° As Obtained from Electron Diffraction and ab Initio Calculations (MP2/6-311+G(2df,2pd))[a]

	$C_s + C_2$		pseudorot. model		ab initio	
	C_s	C_2	C_s	C_2	C_s	C_2
bond distances (Å)						
C_1-C_2	1.523(2)	1.543(2)	1.523(2)	1.544(2)	1.519	1.541
C_2-C_3	1.537(2)	1.529(2)	1.537(2)	1.529(2)	1.535	1.527
C_3-C_4	1.552(3)	1.528(3)	1.552(3)	1.528(3)	1.554	1.528
q[b]	0.396(11)	0.423(11)	0.400(11)	0.428(11)	0.419	0.450
C_1-Cl_6	1.788(3)	1.783(2)	1.787(3)	1.782(2)	1.794	1.790
C_1-Cl_7	1.770(3)	1.783(2)	1.769(3)	1.782(2)	1.776	1.790
⟨C−H⟩[c]	1.114(5)	1.114(5)	1.114(5)	1.114(5)	1.088	1.089
bond angles (deg)						
$C_1-C_2-C_3$	104.2(5)	104.9(6)	104.3(5)	105.0(6)	103.2	104.1
$C_2-C_3-C_4$	105.8(3)	102.7(5)	105.7(3)	102.7(5)	105.7	102.1
$C_5-C_1-C_2$	103.4(9)	106.0(9)	103.0(9)	105.5(9)	103.5	106.3
Cl−C−Cl	108.3(3)	107.6(3)	108.6(3)	107.9(3)	109.0	108.1
$H-C_2-H$	104.1(26)	104.1(26)	104.6(26)	104.6(26)	108.5	108.3
$H-C_3-H$	104.1(26)	104.1(26)	104.6(26)	104.6(26)	107.4	108.1
β_6[d]	122.3(7)	126.2(2)	121.3(8)	126.1(1)	122.1	125.9
β_7[e]	129.3(8)	126.2(2)	130.1(9)	126.1(1)	128.9	125.9
α[f]	39.5(9)		39.9(9)		42.2	
dihedral angles (deg)						
$C_1-C_2-C_3-C_4$	−24.0(7)	35.3(9)	−24.4(7)	35.8(9)	−25.3	37.3
$C_4-C_5-C_1-C_2$	−39.2(10)	−13.5(4)	−39.6(10)	−13.7(4)	−41.7	−14.3
$C_2-C_3-C_4-C_5$	0.0(−)	−43.7(9)	0.0(−)	−44.1(9)	0.0	−46.5

[a] Errors in parentheses include the contributions from the estimated uncertainties of the fixed parameters. [b] Puckering amplitude for the ring. [c] Average value. [d] Angle between the bond Cl_6-C_1 and the plane $C_5C_1C_2$. [e] Angle between the bond Cl_7-C_1 and the plane $C_5C_1C_2$. [f] Angle between the $C_5C_1C_2$ plane and $C_2C_3C_4C_5$ plane (flap angle).

TABLE 10: Optimized Geometrical Parameters of Monochlorocyclopentane (MClCP) and Monofluorocyclopentane (MFCP) As Predicted by Different Levels of Theory

	MClCP				MFCP			
	axial		equatorial		axial		equatorial	
parameter	B3PW91 /6-311 +G(df,pd)	MP2 /6-311 +G(2df,2pd)	B3PW91 /6-311 +G(df,pd)	MP2 /6-311 +G(2df,2pd)	B3PW91 /6-311 +G(df,pd)	MP2 /6-311 +G(2df,2pd)	B3PW91 /6-311 +G(df,pd)	MP2 /6-311 +G(2df,2pd)
bond distances (Å)								
C_1-C_2	1.521	1.520	1.521	1.519	1.518	1.513	1.520	1.516
C_2-C_3	1.538	1.537	1.537	1.536	1.539	1.538	1.536	1.534
C_3-C_4	1.549	1.550	1.553	1.554	1.550	1.551	1.555	1.555
q[a]	0.378	0.411	0.414	0.441	0.375	0.405	0.401	0.430
C_1-H_6	1.089	1.086	1.092	1.090	1.094	1.089	1.097	1.093
$C_1-Cl(F)_7$	1.822	1.801	1.802	1.784	1.402	1.400	1.390	1.388
⟨C−H⟩[b]	1.092	1.089	1.092	1.089	1.092	1.088	1.093	1.089
bond angles (deg)								
$C_1-C_2-C_3$	104.8	104.0	103.1	102.6	104.7	103.7	103.6	102.9
$C_2-C_3-C_4$	105.8	105.6	105.9	105.6	105.9	105.6	105.9	105.5
$C_5-C_1-C_2$	103.5	102.9	103.8	103.1	104.0	103.7	103.9	103.4
Cl(F)-C−H	104.6	105.9	104.9	106.1	106.4	107.0	106.4	107.0
$H-C_2-H$	107.4	108.0	107.7	108.1	107.5	108.1	107.7	108.2
$H-C_3-H$	106.9	107.3	106.7	107.0	106.8	107.2	106.5	106.9
β_6[c]	131.3	131.4	125.3	124.4	131.6	132.5	125.8	123.3
β_7[d]	124.0	122.8	129.8	129.5	122.0	120.6	127.9	127.7
α[e]	37.8	41.0	41.7	44.5	37.6	40.9	40.4	43.5
dihedral angles (deg)								
$C_1-C_2-C_3-C_4$	23.1	25.0	24.9	26.5	22.8	24.6	24.2	25.9
$C_4-C_5-C_1-C_2$	37.6	40.7	41.1	43.7	37.4	40.5	40.4	42.8
μ[f]	2.33	2.36	2.44	2.53	1.99	2.10	2.14	2.30

[a] Puckering amplitude for the ring, calculated with the program RING.[12,13] [b] Average value. [c] Angle between the bond H_6-C_1 and the plane $C_5C_1C_2$. [d] Angle between the bond $Cl(F)_7-C_1$ and the plane $C_5C_1C_2$. [e] Angle between the $C_5C_1C_2$ plane and the $C_2C_3C_4C_5$ plane (flap angle). [f] Dipole moment.

less speculatively to rationalize the higher stability of the axial conformer in comparison to the equatorial one in MClCP by invoking dipole−dipole interaction between the C−Cl bond dipole and the ring dipole. It is conceivable that this kind of dipolar interaction might be responsible for the difference between the axial and equatorial C−X (X = F, Cl, Br) bond lengths in the investigated molecules. It may also be of interest to indicate that the C−Cl bond is shortened by about 0.007 Å on going from MClCP to DClCP, and the C−F bond in DFCP decreases by about 0.027 Å in comparison to MFCP. This bond contraction with increasing halogen substitution has commonly been attributed to the negative hyperconjugation effect. However, we would like rather to ascribe this bond shortening simply to increasing bond ionicity with increasing halogen substitution and subsequent Coulombic attractive interaction between the negatively charged halogen atoms and the increasingly more

TABLE 11: Atomic Charges As Obtained from Natural Population Analysis (NPA) and Mullikan Population Analysis (MPA) for 1,1-Dichlorocyclopentane (DClCP)

	NPA				MPA			
	C_s symmetry		C_2 symmetry		C_s symmetry		C_2 symmetry	
atom	B3PW91 /6-311 +G(df,pd)	MP2 /6-311 +G(2df,2pd)	B3PW91 /6-311 +G(df,pd)	MP2 /6-311 +G(2df,2pd)	B3PW91 /6-311 +G(df,pd)	MP2 /6-311 +G(2df,2pd)	B3PW91 /6-311 +G(df,pd)	MP2 /6-311 +G(2df,2pd)
C_1	−0.063	−0.016	−0.064	−0.018	0.724	1.347	1.562	1.812
$C_{2,5}$	−0.434	−0.365	−0.433	−0.364	−0.647	−0.242	−1.049	−0.424
$C_{3,4}$	−0.403	−0.339	−0.398	−0.335	−0.497	−0.029	−0.406	0.001
Cl_6	−0.028	−0.052	−0.019	−0.042	−0.240	−0.528	−0.134	−0.442
Cl_7	−0.002	−0.024	−0.019	−0.042	0.171	−0.208	−0.134	−0.442
H_8	0.233	0.200	0.227	0.192	0.208	−0.011	0.216	0.002
H_9	0.223	0.186	0.235	0.202	0.210	−0.007	0.209	−0.007
H_{10}	0.215	0.184	0.216	0.184	0.214	0.000	0.184	−0.024
H_{11}	0.213	0.180	0.204	0.171	0.185	−0.016	0.199	−0.013

positively charged carbon atom. The smaller effect on the C−Cl bond is due to the smaller difference in the electronegativity between chlorine and carbon. This kind of rationalization is fully supported by the atomic charges we obtained from the natural population analysis (NPA) as shown in Tables 11, S5, S6, S8, and S10.

We also conducted natural population analysis (NPA)[26−29] and Mulliken population analysis (MPA)[30] for DFCP, DClCP, DBrCP, and their monohalogenated derivatives. In addition, we performed charge distribution analysis on monoethynylcyclopentane (MECP) in its axial and equatorial form. For brevity only the NPA and MPA atom charges for DClCP are shown in Table 11. All other NPA and MPA result, which we obtained for a variety of monosubstituted cyclopentanes, are available as Supporting Information (Tables S5−S11).

On many occasions it has been demonstrated[27,31,32] that the NPA method has substantial advantages over the MPA procedure and avoids various deficiencies incorporated in the latter population analysis. The most aggravating disadvantage of the MPA, however, is its sensitivity to variation of the basis set.[29,32−35] A comparison between the NPA and MPA atom charges for DClCP (Table 11) and DFCP (Tables S6 and S7) clearly visualizes the dependency of the MPA method on the level of theory and the size of the basis set. As is shown in Table 11 (and Tables S7, S9, and S11), besides the evident fluctuation of the atom charges with the variation of the basis set there are instances where the atom charges at some atoms even reverse their signs.

It is interesting to note that the dipole moment does not change noticeably upon going from DClCP to DFCP and DBrCP (C_s and C_2 symmetry) and it decreases only slightly by about 0.2 D on moving from MBrCP to MClCP and MFCP (2.52, 2.36, and 2.12 D, respectively).

Aside from the dependency of the ring C−C bond distances on the phase angle ϕ it is perhaps crucial to lend some attention to the role of the number and kind of substituents by the determination of the ring geometry. From the results shown in Tables 1 and 10 and the results for MBrCP and DBrCP, which are not listed in this paper, it can be generally concluded that the ring parameters are little affected by the variation of the substituent and by the successive halogenation except in the case of the fluoro derivatives. For instance, the C1−C2 bond length in the axial form of MFCP, MClCP, and MBrCP is 1.516, 1.521, and 1.522 Å, respectively, as predicted by the MP2/6-311++G(df,pd) procedure (not shown in this work). Using the same ab initio method we obtained for the C_s conformer of DCCP, DFCP, DClCP, and DBrCP a C_1-C_2 bond length of 1.546, 1.513, 1.523, and 1.523 Å, respectively. It is noteworthy that all other C−C bond lengths as well as all endocyclic valence angles remain almost unaffected by the variation of the substituents (in the mono- and disubstituted series alike). The only exception is found in DFCP where the $C_5-C_1-C_2$ angle widens by approximately 1.8° in comparison to all other compounds. The pronounced variation of the C_1-C_2 bond length and the small change of the remaining C−C bonds with the alternation of the electronegativity of the substituent are mirrored in the NPA charge distribution shown in Tables 11, S6, S8, and S10 and in those values for MBrCP and DBrCP, which are not shown in this work. The most dramatic changes of the charge density occur at the anchor atom C_1 while the charges at the other carbon atoms vary only slightly.

Scrutinizing the behavior of the puckering angle α reveals that consistently all ab initio methods we used demonstrate that the puckering angle increases upon moving from the axial form of MClCP to DClCP (Tables 1 and 11). The variation of this angle in the case of the fluorine counterparts is, however, negligible (less than 1°). In contrast, this angle widens by about 2° to 3° in the equatorial form of MClCP in comparison to DClCP. This variation of the puckering angle α parallels the behavior of the puckering amplitude q. The correlation between these two magnitudes has been discussed above.

The following general conclusion emerges from the data in Table 7: It is discernible that in all cases displayed in this table there is an apparent jump in the ΔE values on going from the DFT method to the MP2 method and in some cases the conformational preferability is even reversed. For instance, the comparison of the ΔE values obtained from B3LYP/6-311+G(df,pd) and MP2/6-311+G(df,pd) for the mono- as well as for the disubstituted cyclopentanes (particularly for DClCP and DBrCP) distinctly confirms this observation. A closer consideration of the energy differences in Table 7 also reveals the following: On moving from MFCP to MClCP, MBrCP, MCCP, and MECP the predominant axial conformer becomes constantly less favorable in comparison with the equatorial conformer. The decrease of the stability of the axial conformer from MFCP to MClCP and MBrCP parallels the decrease of the electronegativity of the halogen atoms F = 4.00,[36] Cl = 3.07,[36] and Br = 2.81[36] and thus demonstrates a correlation between the conformational stability within this series and the electronegativity of the substituent. However, such a relationship does not hold for MCCP and MECP since in these cases the percentage of axial form continues to decrease although the electronegativities for C≡CH and C≡N are 2.66, and 2.69,[37] respectively. This, however, is not particularly surprising since these electron-rich moieties exhibit additional electronic interaction since they are regarded to be strong π- and σ-electron acceptors and weak

TABLE 12: Ring Puckering Amplitude *q* (Å) for MBrCP, Monoethynylcyclopentane (MECP), and DBrCP As Obtained from ab Initio Calculations on Various Levels of Theory

	MBrCP		MECP		DBrCP		cyclopentane		
method	ax	eq	ax	eq	C_s	C_2	C_1	C_2	C_s
B3LYP/6-311+G(df,pd)	0.368	0.411	0.403	0.409	0.385	0.416			
MP2/6-311G(d,p)	0.405	0.437	0.441	0.435	0.416	0.451			
MP2/6-311+G(d,p)			0.439	0.434					
MP2/6-311++G(d,p)	0.403	0.438			0.415	0.451			
MP2/6-311+G(df,pd)	0.405	0.435	0.436	0.432	0.416	0.449	0.424	0.424	0.424
MP2/6-311++G(df,pd)	0.406	0.436	0.437	0.432	0.416	0.449			
MP2/6-311++G(2df,2pd)	0.406	0.442					0.430	0.430	0.430

electron donors as well. Another possible rationalization for the steadily increasing occurrence of the axial conformer within the mono derivatives upon going from the bromo to chloro and fluoro derivatives (Table 7) is the aforementioned dipole−dipole interaction between the C−X bond dipole and the ring dipole.

From Table 7 it is furthermore apparent that the C_2 conformer of DFCP is slightly more stable than the C_s conformer whereas in DCCP, DClCP, and DBrCP the C_s form is significantly more stable than the C_2 form. This interesting conformational interconversion is most likely due to the declining electronegativity of the substituents C≡N, Cl, and Br in comparison to the F atom.

In addition to the puckering amplitudes displayed in Tables 1 and 10 for DFCP, DClCP, and their monosubstituted derivatives we calculated the ring puckering amplitude, *q*, for axial and equatorial conformers of MBrCP, MECP, and MCCP, as well as for DCCP and DBrCP (C_2 and C_s forms) (Table 12). Furthermore, we computed the puckering amplitudes for the probable C_1, C_2, and C_s conformations (obviously $q = 0$ for the D_{5h} form) of the parent molecule cyclopentane (Table 12). From all these values it is evident that there is a general noticeable increase of the *q* values upon going from the DFT method to the perturbation method. This trend parallels the tendency we observed by the consideration of the ΔE values listed in Table 7. Inspection of the *q* values in Tables 1, 10, and 12 reveals that while the equatorial form is significantly more puckered than the axial form, the difference between the *q* values for the equatorial and axial forms in MECP, however, is almost negligible. In contrast, there is a noticeable increase of the *q* values in going from the mono- to the disubstituted cyclopentanes.

Of interest is to compare the puckering parameter, *q*, for the substituted cyclopentanes we discussed so far and for the freely pseudorotating parent molecule cyclopentane. Before carrying out this comparison, however, we would like to point out that the C_1, C_2, and C_s forms of cyclopentane exhibit the same puckering displacement of 0.424 Å as predicted by the MP2/6-311+G(df,pd) method. More or less conspicuously, the values for the total energy for all three nonplanar conformations are almost equal. It should also be mentioned that almost three decades ago Cremer and Pople[13] published the *q* values for various five-membered ring systems, among them cyclopentane. Using the STO-3G and HF/4−31 methods they obtained for cyclopentane a puckering amplitude of $q = 0.37$ and 0.39 Å, respectively. These values are evidently smaller than is suggested by the level of theory we applied. This deviation becomes rather larger when we compare these values with the magnitude of 0.430 Å, which has been provided by the MP2/6-311++G(2df,2pd) method. From this increase in the value for the puckering amplitude it can be concluded that the augmentation of the basis set by incorporating polarization and diffusion functions leads to a larger value of the puckering displacement. This finding is in accord with the prediction by Cremer and Pople.[13] These authors suggested that the addition of polarization functions would influence the degree of puckering. Interestingly, while the value of 0.424 Å is lower than that which was determined many years ago by means of electron diffraction of 0.438 Å,[38] the value of 0.430 Å, however, agrees nicely with the experimental one. From the comparison of both *q* values we obtained for cyclopentane of 0.424 and 0.430 Å with those for the substituted derivatives shown in Tables 1, 10, and 12 it can be decisively noticed that these values lie between the values for puckering amplitudes of the axial and equatorial conformers and between the values for the C_s and C_2 symmetry in the case of the geminally substituted compounds. It remains to note that the experimentally determined puckering amplitude for DClCP (Table 9) of 0.402 Å is considerably smaller than that for cyclopentane of 0.438 Å.

Finally, it is interesting to note that the experimental values of the flap angles α of 39.9° (Table 9) and 41.6° [1] for DClCP and DCCP, respectively, are different. This result is also supported by all computational methods we applied.

Summary and Conclusions

The following principal conclusions can be drawn from this study:

(1) The experimental electron diffraction intensities could be reasonably reproduced by using a two-conformer static model with C_s and C_2 symmetry. Also a proper fit could be achieved by applying a C_1 static model.

(2) The best agreement with the electron diffraction data was achieved by applying a large-amplitude treatment and a potential function, which properly describes the hindered pseudorotational motion in DClCP of the form

$$V(\phi) = {}^1/_2V_2(1 - \cos 2\phi) + {}^1/_2V_4(1 - \cos 4\phi) + {}^1/_2V_6(1 - \cos 6\phi)$$

(3) We could show that there is an inherent correlation between the fluctuation of the charge density distribution throughout the ring in DClCP and thus its geometric parameters and the phase angle ϕ during the pseudorotation. This correlation has been described by evaluating an adequate density distribution function.

(4) Appropriate equations have been developed to characterize the dependency of the geometry parameters on the pseudorotational parameter ϕ.

(5) Simple relationships have been found between the phase angle ϕ and the flap angle α for the envelope C_s conformation on one hand and the twist angle τ for the C_2 (half-chair) conformer on the other hand.

(6) The ab initio results obtained from various methods and different basis sets for a variety of mono and geminally halogenated cyclopentanes have shown that the ring parameters

remain almost unaffected except the fluoro derivatives exhibit slight variations.

(7) Upon going from MFCP to MClCP and MBrCP the predominant axial conformer becomes constantly less favorable in comparison with the equatorial conformer. This behavior parallels the decrease of the electronegativity of the halogen atoms. This demonstrates a correlation between the conformational stability within this series and the electronegativity of the substituent. Due to the particular electronic interaction of the C≡CH and the C≡N moieties as strong π- and σ-electron acceptors and weak electron donors MCCP and MECP do not obey this correlation.

(8) The C_2 conformer of DFCP is slightly more stable than the C_s conformer. In contrast, the C_s form is significantly more stable than the C_2 form for DClCP and DBrCP. This interesting conformational interconversion may be attributed to the declining electronegativity of the substituents Cl and Br in comparison to the F atom.

(9) A significant increase of the ring puckering amplitude, q, has been observed on going from the axial to the equatorial form within the monosubstituted cyclopentanes MFCP, MClCP, MBrCP, MCCP, and MECP. A similar trend for the puckering amplitude is apparent upon proceeding from the C_s to the C_2 form along the corresponding geminally substituted series. The computed ring puckering amplitude for the parent molecule cyclopentane of 0.424 Å lies between the puckering amplitudes for the axial and equatorial forms within the monosubstituted derivatives and between the puckering amplitudes for the C_s and the C_2 form along the geminally substituted homologues.

Acknowledgment. M.D. gratefully acknowledges the financial support from the Fonds der Chemischen Industrie.

Supporting Information Available: Intramolecular atomic distances and calculated corrections ($r_a - r_\alpha$) for 1,1-dichlorocyclopentane at phase angle $\phi = 180°$; additional results of theoretical calculations on molecular geometry and atomic charges of mono- and 1,1-dihalogenated cyclopentanes; and scattering intensities from the diffraction experiment. This material is available free of charge via the Internet at http://pubs.acs.org.

References and Notes

(1) Dakkouri, M.; Typke, V. *J. Mol. Struct.* **2002**, *612*, 181−197.
(2) Domnin, N. A.; Obscchalova, N. V.; Kolinskii, R. C. *Zh. Obshch. Khim.* **1961**, *31*, 2768.
(3) Typke, V.; Dakkouri, M.; Oberhammer, H. *J. Mol. Struct.* **1978**, *44*, 85−96.
(4) Oberhammer, H.; Gombler, W.; Willner, H. *J. Mol. Struct.* **1981**, *70*, 273.
(5) Haase, J. *Z. Naturforsch., A* **1970**, *25*, 936−945.
(6) Frisch, M. J.; Trucks, G. W.; Schlegel, H. B.; Scuseria, G. E.; Robb, M. A.; Cheeseman, J. R.; Zakrzewski, V. G.; Montgomery, J. A., Jr.; Stratmann, R. E.; Burant, J. C.; Dapprich, S.; Millam, J. M.; Daniels, A. D.; Kudin, K. N.; Strain, M. C.; Farkas, O.; Tomasi, J.; Barone, V.; Cossi, M.; Cammi, R.; Mennucci, B.; Pomelli, C.; Adamo, C.; Clifford, S.; Ochterski, J.; Petersson, G. A.; Ayala, P. Y.; Cui, Q.; Morokuma, K.; Malick, D. K.; Rabuck, A. D.; Raghavachari, K.; Foresman, J. B.; Cioslowski, J.; Ortiz, J. V.; Baboul, A. G.; Stefanov, B. B.; Liu, G.; Liashenko, A.; Piskorz, P.; Komaromi, I.; Gomperts, R.; Martin, R. L.; Fox, D. J.; Keith, T.; Al-Laham, M. A.; Peng, C. Y.; Nanayakkara, A.; Gonzalez, C.; Challacombe, M.; Gill, P. M. W.; Johnson, B.; Chen, W.; Wong, M. W.; Andres, J. L.; Gonzalez, C.; Head-Gordon, M.; Replogle, E. S.; Pople, J. A. *Gaussian 98*, Revision A.7; Gaussian, Inc.: Pittsburgh, PA, 1998.
(7) Hehre, W. J. *SPARTAN*, Release 5.0.3; Wavefunction, Inc.: Irvine, CA, 1994.
(8) *MOLPRO* is a package of ab initio programs designed by H.-J. Werner and P. J. Knowles, R. D. Amos, A. Bernhardsson, A. Berning, P. Celani, D. L. Cooper, M. J. O. Deegan, A. J. Dobbyn, F. Eckert, C. Hampel, G. Hetzer, P. J. Knowles, T. Korona, R. Lindh, A. W. Lloyd, S. J. McNicholas, F. R. Manby, W. Meyer, M. E. Mura, A. Nicklass, P. Palmieri, R. Pitzer, G. Rauhut, M. Schütz, U. Schumann, H. Stoll, A. J. Stone, R. Tarroni, T. Thorsteinsson, and H.-J. Werner.
(9) Fuchs, B. In *Topics in Stereochemistry*; Eliel, E. L., Allinger, N. L., Eds.; John Wiley & Sons: New York, 1978; Vol. 10, p 1.
(10) Laane, J. In *Vibrational Spectra and Structure*; Durig, J. R., Ed.; Consultants Bureau: New York, 1972, Vol. 1, p 25.
(11) Strauss, H. L. *Annu. Rev. Phys. Chem.* **1983**, *34*, 301.
(12) Cremer, D., Program *RING*, QCPE Program No. 288, Indiana University: Bloomington, IN, 1975.
(13) Cremer, D.; Pople, J. A. *J. Am. Chem. Soc.* **1975**, *97*, 1358−1367.
(14) Kilpatrick, J. E.; Pitzer, K. S.; Spitzer, R. *J. Am. Chem. Soc.* **1947**, *69*, 2483−2488.
(15) Skancke, P. N.; Fogarasi, G.; Boggs, J. E. *J. Mol. Struct.* **1980**, *62*, 259.
(16) Dakkouri, M.; Typke, V. *J. Mol. Struct.* **1994**, *320*, 13−28.
(17) ter Brake, J. H. M.; Mijlhoff, F. C. *J. Mol. Struct.* **1978**, *77*, 109−112.
(18) Dakkouri, M.; Typke, V.; Bitschenauer, R. *J. Mol. Struct.* **1995**, *355*, 239−263.
(19) Hilderbrandt, R. L.; Shen, Q. *J. Phys. Chem.* **1982**, *86*, 587−593.
(20) Hilderbrandt, R. L.; Leavitt, H.; Shen, Q. *J. Mol. Struct.* **1984**, *116*, 29−37.
(21) (a) Typke, V.; Dakkouri, M.; Schiele, M. *Z. Naturforsch.* **1980**, *35a*, 1402−1407. (b) Dakkouri, M.; Typke, V. *J. Mol. Struct.* **2000**, *550−551*, 349−364.
(22) Kuchitsu, K.; Cyvin, S. J. In *Molecular Structures and Vibrations*; Cyvin, S. J., Ed.; Elsevier: Amsterdam, The Netherlands, 1972; p 183.
(23) Vilkov, L. V.; Penionzhkevich, N. P.; Brunvoll, J.; Hargittai, I. *J. Mol. Struct.* **1978**, *43*, 109−115.
(24) Loyd, R. C.; Mathur, S. N.; Harmony, M. D. *J. Mol. Spectrosc.* **1978**, *72*, 359−371.
(25) Groner, P.; Lee, M. J.; Durig, J. R. *J. Phys. Chem.* **1991**, *72*, 3315−3321.
(26) Foster, J. P.; Weinhold, F. *J. Am. Chem. Soc.* **1980**, *102*, 7211.
(27) Reed, A. E.; Weinstock, R. B.; Weinhold, F. *J. Chem. Phys.* **1985**, *83*, 735.
(28) Reed, A. E.; Weinhold, F. *J. Chem. Phys.* **1983**, *78*, 4066.
(29) Reed, A.; Schleyer, P. v. R. *J. Am. Chem. Soc.* **1990**, *112*, 1434.
(30) Mulliken, R. S. *J. Chem. Phys.* **1955**, *23*, 1833.
(31) Reed, A. E.; Weinhold, F. *J. Chem. Phys.* **1985**, *83*, 1736.
(32) Reed, A. E.; Weinhold, F. *J. Am. Chem. Soc.* **1986**, *108*, 3586.
(33) Dakkouri, M.; Grosser, M. *J. Mol. Struct.* **2002**, *610*, 159.
(34) Baker, J. *Theor. Chim. Acta* **1985**, *68*, 221.
(35) Reed, A.; Weinhold, F.; Weiss, R.; Macheleid, J. *J. Phys. Chem.* **1985**, *89*, 2688.
(36) Mullay, J. *J. Am. Chem. Soc.* **1984**, *106*, 5842.
(37) Boyd, R. J.; Edgecombe, K. E. *J. Am. Chem. Soc.* **1988**, *110*, 4182.
(38) Adams, W. J.; Geise, H. J.; Bartell, L. S. *J. Am. Chem. Soc.* **1970**, *92*, 5013.